

CAPITAL UNIVERSITY OF SCIENCE AND
TECHNOLOGY, ISLAMABAD



**Synthesis, Characterization and
Pharmacological Evaluation of
Newly Synthesized Benzothiazole
Derivatives**

by

Sadiqa Ghadeer

A thesis submitted in partial fulfillment for the
degree of Master of Philosophy

in the

Faculty of Pharmacy

Department of Pharmaceutical Chemistry

2025

Copyright © 2025 by Sadiqa Ghadeer

All rights reserved. No part of this thesis may be reproduced, distributed, or transmitted in any form or by any means, including photocopying, recording, or other electronic or mechanical methods, by any information storage and retrieval system without the prior written permission of the author.

The journey of my work would have lacked direction, my efforts would have been in vain, and any recognition would have felt empty without the unwavering love, support, and prayers of my parents. With the successful completion of my thesis,

I whole heartedly dedicate this research endeavor to my beloved father and mother, as well as to my all family members, whose encouragement has been my greatest strength.



CERTIFICATE OF APPROVAL

Synthesis, Characterization and Pharmacological Evaluation of Newly Synthesized Benzothiazole Derivatives

by

Sadiqa Ghadeer

(Registration No: MPH233026)

THESIS EXAMINING COMMITTEE

S. No.	Examiner	Name	Organization
(a)	External Examiner	Dr. Kishwar Sultana	Iqra Uni, Islamabad
(b)	Internal Examiner	Dr. Mehboob Alam	CUST, Islamabad
(c)	Supervisor	Dr. Reem	CUST, Islamabad

Dr. Reem

Thesis Supervisor

October, 2025

Dr. Reem

Head

Dept. of Pharmaceutical Chemistry

October, 2025

Dr. Muzaffar Abbas

Dean

Faculty of Pharmacy

October, 2025

Author's Declaration

I, **Sadiqa Ghadeer** hereby state that my M.Phil thesis titled “**Synthesis, Characterization and Pharmacological Evaluation of Newly Synthesized Benzothiazole Derivatives**” is my own work and has not been submitted previously by me for taking any degree from Capital University of Science and Technology, Islamabad or anywhere else in the country/abroad.

At any time if my statement is found to be incorrect even after my graduation, the University has the right to withdraw my M.Phil Degree.



(Sadiqa Ghadeer)

Registration No: MPH233026

Plagiarism Undertaking

I solemnly declare that research work presented in this thesis titled “**Synthesis, Characterization and Pharmacological Evaluation of Newly Synthesized Benzothiazole Derivatives**” is solely my research work with no significant contribution from any other person. Small contribution/help wherever taken has been duly acknowledged and that complete thesis has been written by me.

I understand the zero tolerance policy of the HEC and Capital University of Science and Technology towards plagiarism. Therefore, I as an author of the above titled thesis declare that no portion of my thesis has been plagiarized and any material used as reference is properly referred/cited.

I undertake that if I am found guilty of any formal plagiarism in the above titled thesis even after award of M.Phil Degree, the University reserves the right to withdraw/revoke my M.Phil degree and that HEC and the University have the right to publish my name on the HEC/University website on which names of students are placed who submitted plagiarized work.



(Sadiqa Ghadeer)

Registration No: MPH233026

Acknowledgement

In the name of Allah, the Most Gracious, the Most Merciful. May peace and blessings be upon His messenger, Prophet Muhammad (peace be upon him). I seek help from none but Allah, for He alone guides us in both our worldly and spiritual pursuits.

First and foremost, I would like to express my heartfelt gratitude to my supervisor, Dr. Reem. Her guidance, encouragement, and unwavering support have been instrumental throughout my research journey. I truly value the trust she placed in me, her insightful feedback, and her ability to uplift my spirit during challenging times. This research would not have been possible without her direction and mentorship. I pray for her continued health and wish her abundant happiness and success.

Lastly, I would like to extend my sincere thanks to Capital University of Science and Technology for providing the resources, facilities, and a supportive academic environment that enabled me to conduct this research effectively.

(Sadiqa Ghadeer)

Abstract

Benzothiazole derivatives represent a privileged scaffold in medicinal chemistry owing to the variety of structure and extensive pharmacological activity, encompassing antibacterial, anticancer, anti-inflammatory, and antioxidant properties. This study focuses on the synthesis, characterization, and biological evaluation of newly synthesized benzothiazole derivatives, *N*-(1,3-benzothiazol-2-yl)-2-chloroacetamide (F1) and *N*-(1,3-benzothiazol-2-yl)-2-[(2,3-dihydro-1,3-benzothiazol-2-yl)amino]acetamide (F2). The synthesis involved a two-step process: (1) 2-aminobenzothiazole condensation with monochloroacetyl chloride to yield F1, followed by (2) refluxing F1 with 2-aminobenzothiazole to obtain F2. Both compounds were purified via column chromatography and characterized using IR, $^1\text{H}/^{13}\text{C}$ NMR, confirming high purity and structural integrity. F2 exhibited superior bioactivity in pharmacological assays. Molecular docking revealed strong binding affinity of F-2 (-7.5 kcal/mol) toward COX-2 (PDB: 3LN1), surpassing F1 (-6.8 kcal/mol) and approaching diclofenac (-8.0 kcal/mol). The protein-ligand complex molecular dynamic simulation revealed stable binding interactions, with the ligand exhibiting low RMSD fluctuations ($\sim 1\text{--}2$ Å) and key residues (e.g., *HIS*₉₀, *SER* – 300) maintaining consistent contacts. The system equilibrated effectively, demonstrating structural integrity and potential for further drug development. *In-vivo* studies demonstrated F2's potent analgesic activity by significantly reducing thermal hyperalgesia (hot plate test) and comparable to diclofenac at 3 hours. F2 exhibited anti-inflammatory effects by reducing paw edema to 3.21 ± 0.2 mm ($p < 0.001$ vs control), outperforming Diclofenac at 3 hours (3.36 ± 0.06 mm). F2 also displayed dose-dependent antioxidant activity ($\text{IC}^{50} = 302.3 \mu\text{g}/\text{mL}$), nearing ascorbic acid ($226.9 \sim \mu\text{g}/\text{mL}$), with 90.5% radical scavenging at $1000 \sim \mu\text{g}/\text{mL}$. Toxicity studies in mice (10 mg/kg, 14 days) confirmed F2's safety, with no behavioral abnormalities, organ damage, or histopathological changes.

Collectively, F2 emerges as a multifunctional therapeutic candidate with dual anti-inflammatory-antioxidant properties, low toxicity, and efficacy comparable to

standard drugs. These findings underscore the benzothiazole scaffold's potential in developing novel agents for oxidative stress-related and inflammatory disorders.

Contents

Author's Declaration	iv
Plagiarism Undertaking	v
Acknowledgement	vi
Abstract	vii
List of Figures	xii
List of Tables	xiii
Abbreviations	xiv
1 Introduction	1
1.1 The Role of Benzothiazole Derivatives in Drug Discovery	4
1.2 Innovative Approaches to the Synthesis of C-2-Substituted Benzothiazoles	6
1.3 Rationale of Current Research Work	13
1.4 Aims and Objectives	13
2 Literature Review	15
2.1 Novel Benzothiazole Based Cytotoxic Agents and Their Mechanisms	15
2.2 Novel Substituted Benzothiazoles as Potent Anti-Inflammatory Candidates	16
2.3 Benzothiazole Derivatives Emerge as a Strong Pain-Relieving Agent	17
2.4 Mechanistic Insights into Benzothiazole Based Antimicrobial Action	17
2.5 Novel Benzothiazole Compounds as a Promising Antidiabetic Agent	18
2.6 Benzothiazole Derivatives as Versatile Central Nervous System Modulators	18

2.7	Benzothiazole Analogues Demonstrate Promising Antiepileptic Potential	19
2.8	Phenolic Groups Drive Antioxidant Activity in Novel Benzothiazole Compounds	20
2.9	Benzothiazole Compounds Exhibit Remarkable Activity against Influenza A and B Strains	20
2.10	2-Imidazoliny-Benzothiazoles Show Selective DNA-Binding Activity	21
2.11	Novel Benzothiazole-Based Diuretic Agent	21
2.12	2-Amino Benzothiazole Derivatives Protect Against Oxidative Damage	22
2.13	<i>In Silico</i> Studies of Benzothiazole Derivatives	22
3	Materials and Methods	27
3.1	Materials and Methods	27
3.1.1	Chemicals and Solvent	27
3.1.2	Software's for <i>In silico</i> Studies	27
3.2	Methodology	27
3.2.1	Experimental	27
3.2.1.1	<i>General Scheme for the Synthesis of 2,2 chloroacetoaminobenzothiazole (F1)</i>	28
3.2.1.2	<i>General Scheme for Synthesis of N,N'-bis[(2,3-dihydro-1,3-benzothiazol-2-yl)] (F2)</i>	28
3.2.2	<i>In Silico</i> Studies	30
3.2.2.1	<i>ADMET Properties of Synthesized Compounds</i>	30
3.2.2.2	<i>Molecular Docking Studies</i>	30
3.2.2.2.1	<i>Retrieval of receptors structure from Protein Data Bank</i>	30
3.2.2.2.2	<i>Ligands-Molecular Docking</i>	30
3.2.2.2.3	<i>Structural analysis of target proteins</i>	31
3.2.2.3	<i>Molecular Dynamic Simulation</i>	32
3.2.2.4	<i>Chemoinformatic Properties</i>	32
3.2.3	Pharmacological Evaluation	33
3.2.3.1	<i>In-vitro</i> Assays	33
3.2.3.1.1	Antioxidant Potential Evaluation Using DPPH Assay	33
3.2.3.2	<i>In-vivo</i> Assays	33
3.2.3.2.1	Induction of Carragenan Triggered Inflammatory Pain and Thermal Hyperalgesia Study	33
3.2.3.2.2	Anti-Inflammatory Evaluation of Synthesized Benzothiazole Derivative	34
3.2.3.2.3	Acute Oral Toxicity Profiling	34
4	Results and Discussion	36
4.1	Results and Discussion	36

4.1.1	Experimental	36
4.1.2	^1H NMR (δ , ppm) and ^{13}C NMR (δ , ppm) spectral data of F1	38
4.1.3	^1H NMR (δ , ppm) and ^{13}C NMR (δ , ppm) spectral data of F2	39
4.1.4	Physical data of synthesized compounds	41
4.2	<i>In Silico</i> Studies	42
4.2.1	<i>ADMET</i> Properties	42
4.2.2	<i>Molecular Docking Studies</i>	43
4.2.3	Molecular Dynamic Simulation	45
4.2.3.1	<i>RMSD Analysis</i>	45
4.2.3.2	<i>RMSF Analysis</i>	47
4.2.3.3	<i>Protein-Ligand Contacts</i>	48
4.2.3.4	<i>Ligand Protein Contacts</i>	50
4.2.3.5	<i>Ligand Torsion Profile</i>	51
4.2.4	Cheminformatics Properties of Synthesized Compounds	52
4.3	<i>In Vitro</i> Studies	53
4.3.1	<i>Anti-Oxidant Assay</i>	53
4.4	<i>In Vivo</i> Studies	55
4.4.1	Induction of Carrageenan Triggered Inflammatory Pain and Thermal Hyperalgesia Study	55
4.4.2	Anti-Inflammatory Action of F2 Against Carrageenan Induced Paw Inflammation	56
4.4.3	<i>In Vivo</i> Acute Toxicity Assessment	58
5	Conclusion and Future Prospects	63
	Bibliography	65

List of Figures

1.1	Pharmacological uses of Benzothiazole compounds	6
3.1	RAMACHANDRAN plots for COX-2 (PDB ID: 3LN1).	32
4.1	FTIR Results of F2 Compound	37
4.2	^1H NMR (δ , ppm) of Compound F2	39
4.3	^{13}C NMR (δ ppm) of Compound F2	40
4.4	2D and 3D presentation of binding interactions of F1with the binding site of COX-2 (PDB ID: 3LN1)	44
4.5	2D and 3D presentation of binding interactions of F2 with binding site of COX- 2 (PDB ID: 3LN1).	44
4.6	2D and 3D presentation of binding interactions of Diclofenac with binding site of COX-2 (PDB ID: 3LN1)	44
4.7	RMSD Analysis of F2 Compound with target protein	46
4.8	RMSF Analysis of compound F2 with target protein	47
4.9	Protein –ligand contact of Compound F2	48
4.10	Interaction Fraction for the Compound F2	49
4.11	Ligand protein Contact of Compound F2	51
4.12	The precise interactions between the protein residues and the ligand atoms	51
4.13	Ligand Torsion Profile of Compound F2	52
4.14	Percentage free radical scavenging activity by DPPH for synthesized Compound F1 and F2 (Mean \pm SEM).	54
4.15	Carrageenan-Induced Thermal Hyperalgesia for negative, positive controls, and treatment groups (F1 and F2) n=4, Data (mean \pm SEM) were analyzed by one-way ANOVA with Tukey’s post-hoc test, (p<0.05-0.01 vs control	56
4.16	Anti-Inflammatory activity by Carrageenan-Induced Paw Inflammation fornegative, positive controls, and treatment groups (F1 and F2) n=4, Data (mean \pm SEM) were examined using Tukey’s post-hoc test and one-way ANOVA (p<0.01-0.001 vs control	57
4.17	Histopathology of Vital Organs (heart, stomach, liver, and kidney) of treated animals, compared to control in Acute Toxicity study for synthesized compounds F1 and F2	60

List of Tables

4.1	FT-IR ($\bar{\nu}$ (cm^{-1})) spectral data of F1 and F2 compounds.	37
4.2	Physical properties of F1 and F2	41
4.3	ADMET Properties of synthesized compounds (F1 and F2)	42
4.4	Highest binding affinity of F1, F2, and Diclofenac with COX-2 (PDB ID:3LN1)	43
4.5	Cheminformatics properties of Synthesized Compounds	53
4.6	Effects of Oral Administration of Compounds F1 and F2 on Body Weight, Consumption, and Toxicity Parameters (Mean \pm SEM)	58

Abbreviations

ABTs	Amino Benzothiazoles
ADME	Absorption Distribution Metabolism Excretion
AMPK	Adenosine Monophosphate Activated Protein kinase
ANOVA	Analysis of Variance
ARG	Arginine
CBV4	Coxsackie virus B4
COX	Cyclooxygenase
DCM	Dichloromethane
DMF	Di-methyl formide
DMSO	Dimethyl Sulfoxide
DNA	Deoxyribonucleic acid
DPPH	Diphenyl picrylhydrazyl
FST	Forced swimming tests
FT IR	Fourier Transform Infrared
GO	Graphene oxide
GOLD	Genetic Optimization for Ligand Docking
HAV	Hepatitis A virus
HCV	Hepatitis C virus
HIV	Human Immuno-deficiency Virus
i-PrOH	Iso-Propyl alcohol
LAH	Lithium Aluminium Hydride
NMR	Nuclear Magnetic Resonance
NSAIDS	Non steroidal anti-inflammatory drugs
PABA	Para Amino benzoic acid

PDB	Protein Data Bank
PPAR	Peroxisome proliferator-activated receptor
RMSD	Root Mean Square Deviation
RMSF	Root Mean Square Fluctuation
ROF	Rule of Five
TEA	Triethanolamine
TLC	Thin layer chromatography
TPSA	Topological Polar Surface Area
TST	Tail suspension tests
UBTs	Urea Benzothiazoles
VEGFR	Vascular Endothelial Growth Factor Receptor

Chapter 1

Introduction

Heterocyclic compounds are considered a basic branch of organic chemistry, with roots in medicinal chemistry and organic synthesis [1]. Any member of broad category of organic chemical compounds that have a minimum of one atom of an element except than carbon joined to all or some of their atoms in rings within their molecules [2]. Heterocyclic compounds have gathered a significant amount of their enthusiasm due to their many important biological and medicinal applications and are present in more than 90% of novel drugs [3]. Heterocyclic molecules are found in a variety of naturally occurring substances, such as alkaloids like vinblastine, morphine, reserpine, and antibiotics like cephalosporin and penicillin [4]. Beginning in the 1800s, heterocyclic chemistry developed concurrently with the advancement of organic chemistry. A few significant developments in 1818, Alloxan is separated by Brugnatelli in 1832 from uric acid. Dobereiner breaks down starch using sulfuric acid to make furfural (afuran)1834: Runge acquires bone pyrrole ("fiery oil") through dry distillation in 1906: The function that heterocyclic substances (pyrimidines and purines) play in the human genome is emphasized in the Chargaff's laws explanation [5]. Heterocyclic substances are deemed as a significant category of organic compounds due to their applications in pharmaceuticals and industrial research [6]. Almost all natural products and manufactured organic compounds contain heterocycles, which are versatile molecules that are typically involved in one or more biological activities.

Heterocyclic compounds are atoms arranged in cyclic rings with minimum of one heteroatom. Heteroatoms that are most common are sulfur, nitrogen, and oxygen; however, rings that are heterocyclic and containing additional heteroatoms, like magnesium, iron, and phosphorus, and selenium, are also frequently found [6]. Although there are many heterocyclic substances having rings containing three to six carbons, only those having ring with five or six atoms is the most significant by far. In order to form heterocyclic compounds, an element with two or more valences can contribute from any one of its atoms. These atoms' bond angles are extremely similar to the bond angles of the hybridized C atom, which is why ring compounds containing these atoms and carbon atoms form [7]. Numerous chemical disciplines have been particularly interested in the impact of molecular structure on chemical reactivity, and quantum chemistry computations have been widely used to analyze reaction mechanisms, interpret experimental data, and resolve chemical ambiguities [8]. Heterocycles can display substituents in diverse 3D arrangements around a central scaffold—a key structural feature that the pharmaceutical industry heavily exploits.

Typically, the size, kind, and quantity of heteroatom within the ring determine how heterocyclic compounds are categorized. In nature, nitrogen heterocyclic molecules are more prevalent than other heterocyclic ring systems [9]. Heterocyclic compounds are classified into three primary categories: nitrogen-based compounds such as pyrazole, indole, imidazole, piperidine, and pyridine; sulfur-based compounds including thiazole, thiadiazole, and thiophene; and oxygen-based compounds like benzofuran and oxazolidine. There are two types of heterocyclic derivatives: aromatic and non-aromatic groups [10]. Most commonly used aromatic compounds are homocyclic, meaning they only contain carbon as their backbone. However, there is another class of aromatic compounds that are heterocyclic, meaning that has minimum of a single non-carbon atom, like as an oxygen, nitrogen, or sulfur atom—is present in the backbone structure. Both pyridine and pyrrole are heterocyclic aromatic compound that include nitrogen. Thiophene is a heterocyclic aromatic compound containing sulfur, furan is a heterocyclic aromatic compound containing oxygen [11]. Heterocyclic compounds are characterized as

being aliphatic compounds with one or more heterocyclic atoms in their rings [12]. Cyclic amines, cyclic amides, cyclic ethers, and cyclic thioethers are classifications of aliphatic heterocyclic compounds. Aliphatic heterocycles without double bonds are classified as saturated heterocycles. The primary factor influencing the characteristics of aliphatic heterocycles is ring strain [5]. The reactivity of aromatic heterocycles, which is a result of both the influence of the heteroatoms involved and the reactivity predicted from an aromatic system, is generally typically more intricate, but the non-aromatic systems reactivity is largely analogous to that of their usual non-cyclic equivalents. The primary emphasis of chemistry is on the reactivity of aromatic molecules [13].

Heterocyclic compounds are widely used in various applications; they are primarily utilized as veterinary products, agrochemicals, and pharmaceuticals [14]. In addition to being a crucial structural component in medicinal chemistry, heterocycles are also typically present in substantial proportions in biomolecules. Biomolecules encompass a wide array of essential compounds, including vitamins, enzymes, and natural products. Furthermore, this category extends to biologically active chemicals exhibiting diverse properties, such as anti-inflammatory, antifungal, antibacterial, anticonvulsant, antiallergic, antioxidant, and enzyme inhibitor activities. They also include compounds with herbicidal, anti-HIV, antidiabetic, anticancer, and insecticidal characteristics [15]. The inhibition of yeast growth may be considerably increased if certain locations in the benzene ring have groups comprising nitro, methoxy, trifluoromethyl, and/or halogen. For this reason, when creating target molecules, combining these patterns with heterocycles could expedite the search for novel antifungal medications [16]. It is possible to think of the heterocyclic nucleus found in DNA intercalators as a pharmacophore that is crucial in determining the affinity and selectivity displayed by these substances [17]. Heterocyclic compounds are essential for lead optimization in drug development, which involves methodically modifying first hit compounds to improve their pharmacological characteristics and reduce risks [18]. Pyrazoles, sometimes referred to as azoles, are heterocyclic substances that majority of the time, are used to treat inflammatory conditions like arthritis [19]. Benzothiazole is a desirable scaffold

among many different heterocyclic compounds because of its special and adaptable qualities in the design of experimental drugs. Despite the established Heterocyclic compounds' significance in medicine and synthetic chemistry, in addition to the domain of drug discovery, the synthesis of these compounds is still a challenging task despite their ease of use and practicality [20]. Catalyzed synthetic methods for heterocyclic compounds are very interesting. Examples of few of sustainable catalytic systems are photocatalysts, iodine-catalyzed reactions, electrochemical reactions, and green, innovative methods, as well as the most significant conventional catalytic systems like transition metals and organocatalysts [21].

Current developments in synthetic routes includes transition-metal-catalyzed reactions, classical routes and creative approaches utilizing sustainable and green chemistry principles for the creation of chemicals that are heterocyclic compounds containing nitrogen and sulfur [22]. An ester (S2), hydrazide (S3), and azo dye (S1) are used in a multi-step process to synthesize new heterocyclic compounds [23]. Researchers are experimenting with novel green methods for the creation of heterocyclic substances that focuses on creating synthetic pathways using green chemistry principles that use renewable resources, consume less energy, and generate little waste. The experiments employed safe reaction conditions, alternative, sustainable starting materials, and catalysis [24].

1.1 The Role of Benzothiazole Derivatives in Drug Discovery

Benzothiazole is a heterocyclic compound that contains a thiazole ring fused to a benzene ring. Benzothiazoles are bicyclic heterocyclic compounds consisting of fused benzene and thiazole rings, containing electron-rich nitrogen and sulfur heteroatoms. These structural features make them highly attractive scaffolds in medicinal chemistry and drug development research because to their great medicinal action [25]. Benzothiazole derivatives are commonly found in pharmaceutical

medications and natural products, it has a wide range of pharmacological characteristics, and many of its analogues are structurally diverse, which allows the development of novel pharmaceuticals. The benzothiazole nucleus aids in the synthesis of numerous medicinal products. Although it is linked to a variety of pharmacological characteristics, benzothiazole, a strong pharmacophore and one of the intriguing heterocycles, is crucial to medicinal chemistry [26].

The benzothiazole skeleton constitutes the basis for the chemical structures that comprise certain potent medications, such as riluzole, lentizole, pramipexole, and thioflavin T. Based on its chemical structure, benzothiazole and its derivatives have an abundance of pharmacological potentials. At present, a single molecule with strong pharmacological effect is created by hybridizing two or more pharmacophores [27]. However, the type and location of benzothiazoles within the pharmacological structure dictate their various biological efficacies.

Benzothiazole and its derivatives have already been shown to be sustainable in the phase of water. The amine tautomeric variants of these compounds have been found to be more resilient than their imine tautomeric counter-parts; a reason for this was that the hydrogen atom is positioned more toward the sulfur atom. In contrast to their amine analogue, imine tautomers are unstable because the hydrogen atom in the imine may approach the sulfur atom, increasing the angle between the two nitrogen and carbon atoms [28]. Additionally, these compounds can block enzymes. Enzyme suppression is consequently one of the most extensively utilized strategies for identifying new screening tools for the prompt identification and management of multiple medical concerns.

Benzothiazole derivatives acquired widespread recognition in 2023 and have a several therapeutic uses, encompassing the effective treatment of leishmaniasis, cancer, bacteria, viruses, convulsions, and malaria. In pharmaceutical chemistry, benzothiazole is a malleable nucleus, therefore, this particular molecule must be explored as a therapeutic lead for the generation of distinct biological intermediary in the future [29]. Derivatives of benzothiazoles have lately been explored for potential applications as agents in neurodegenerative diseases. Diagnostics,

that include as selective fatty acid amide hydrolase inhibitors, histamine H2 antagonists, appetite suppressants, and inhibitors of stearoyl-coenzyme a desaturase, orexin, and LTD4 receptors. Novel ideas are propelling the development of medications incorporating BTA that show increased activity, less toxicity, and better diagnostic efficacy [30].

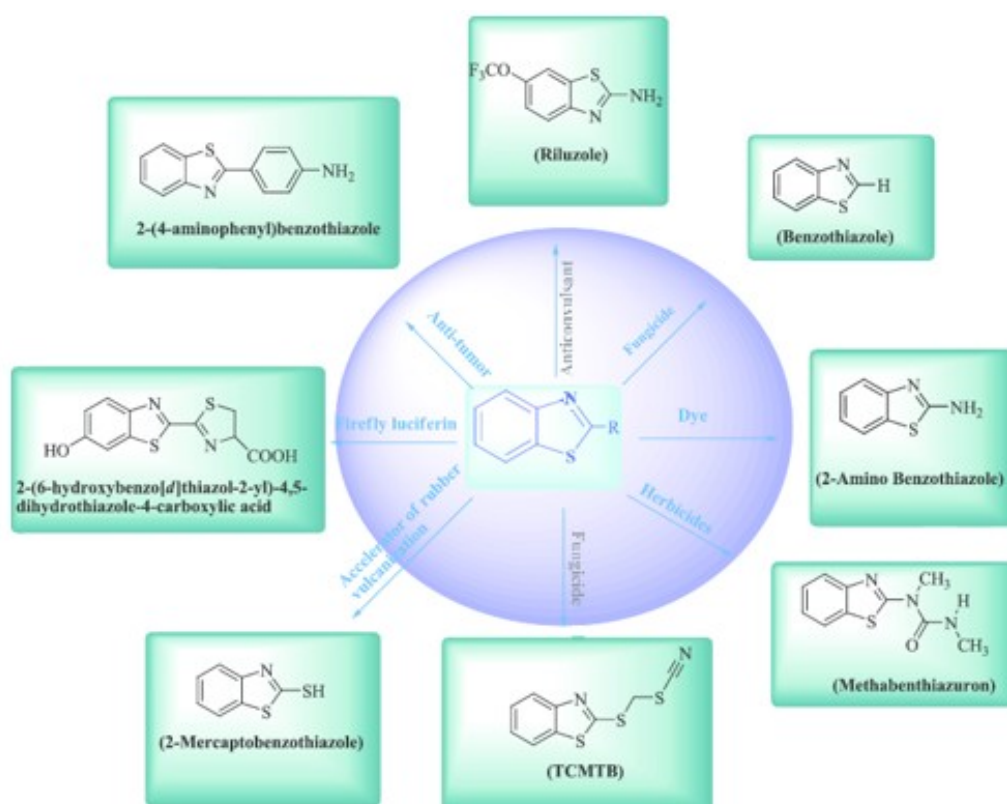


FIGURE 1.1: Pharmacological uses of Benzothiazole compounds

[31]

1.2 Innovative Approaches to the Synthesis of C-2-Substituted Benzothiazoles

There are several published techniques for synthesizing benzothiazole derivatives, but the vast majority of them are impractical because they require strong acidic conditions, higher temperatures, and longer reaction time frames, as well as exorbitant catalysts and solvents. Current developments in the design of compounds with medicinal activity and industrial demand are based on benzothiazole

derivative having C2-Substitutions [32]. Multiple approaches for synthesizing of benzothiazole derivatives are: A. W. Hofmann initially synthesized 1-Mercapto-benzothiazol in an effort to obtain the thiocarbanilide disulphydryl derivative by reacting carbon disulfide with o-aminophenol. One of another method describes a straightforward approach for converting substituted 2-aminobenzothiazoles into 2-azidobenzothiazoles. Benzothiazole bearing amides (A01–A10) were the end products that were prepared in two stages. First, using paraamino benzoic acid (PABA) and 2-amino thiophenol as the starting materials, we synthesized the key intermediate in a satisfactory yield in accordance with the published procedure with minor adjustments. 2-(thio)ureabenzothiazoles [(T)UBTs] are class of compound synthesize by the interaction of carbon disulfide, isocyanates, isothiocyanates, isophosgenes, thiophosgenes, and thiocarbamoyl chlorides with substituted 2-aminobenzothiazoles (ABTs) [33].

Current developments in the green chemistry-related synthesis of benzothiazole compounds involves cyclization reactions utilizing either thioamides or carbon dioxide (CO_2) as starting materials, as well as the condensation of 2-aminobenzenethiol with various compounds such as aldehydes, ketones, carboxylic acids, and acyl chlorides. By using ultrasonic irradiation to condense 2-aminothiophenol with different aromatic aldehydes for 20 minutes at room temperature, benzothiazole derivatives can be produced. The range of yields is 65% to 83% [34]. Using polyphosphoric acid to treat 2-aminothiophenol and substituted aromatic acids offers a good yield and a good way to synthesize 2-substituted benzothiazoles. Equimolar quantities of aniline and ammonium thiocyanate underwent a condensation reaction with bromine acting as a catalyst to produce 2-aminobenzothiazole. *DMSO*/120⁰C, ionic liquid 1-phenyl-methylimidazolium bromide [pmIm] Br, scandium triflate, silica gel, MnO_2/SiO_2 , iodine, citric acid, montmorillonite KSF, copper supported on functionalized MCM-41, cetrimonium bromide (CTAB)/H₂O, and Al_2O_3/Fe_2O_3 were among the catalysts used to enhance the reactions. Cyclization and one-pot coupling of o-substituted anilines with aldehydes, catalyzed by eosin Y, has been established to produce and benzothiazoles derivatives under mild conditions. In contrast to earlier research, the

use of eosin Y as a photocatalyst under substantially enhanced reaction conditions produced the desired compounds in high yields [35].

A variety of methods which employ bromine as a catalyst have been reported recently. In essence, arylthiourea, aniline, and substituted aniline are oxidized with alkali thiocyanate in acid or chloroform resulting in cyclization with bromine. Hegerschoff first reported the cyclization of arylthiourea in chloroform with liquid bromine to yield 2-aminobenzothiazole, a process he developed in the early 1900s prior to its formal synthesis [36]. Employing solvent-free ultrasonic irradiation and a catalytic quantity of LAIL@MNP, for the creation of benzothiazole and benzoxazole a green approach was developed. This method developed 15 benzoxazole and benzothiazole derivatives with moderate to good yields (ranging from 21 to 90%). The Vilsmeier-Haack reaction was used to create two series of pyrazole conjugated benzothiazole derivatives, which were then followed by the Schiff's base formation [37].

N-2'-methoxyphenyl-4-nitrobenzamide was produced via the initial reaction of oanisidine with p-nitrobenzoyl chloride in the benzothiazole synthesis stated by Serdons, K. Next, 2,4-bis(4-methoxyphenyl)-1,3-dithia-2,4-diphosphetane-2,4-disulphide) is Lawesson's reagent was used to transform the amide into the thiobenzamide, a helpful thiation agent that substitutes sulfur for the atoms of carbonyl oxygen in amides, esters, and ketones. It underwent cyclization to produce the 2-(4'-nitrophenyl)-benzothiazole when potassium ferricyanide was added [38]. Piperidine was used as a catalyst in ethanol in order to synthesize a series of chromene derivatives through a multistep synthesis procedure utilizing 1-[3-phenyl prop-2-ene nitrile], dimedone, and 1,3-benzothiazole. Aldehyde-benzothiazole Knoevenagel condensation was found to be the first step in the reaction. This was eventually removed to produce 3-(aryl)acrylonitrile, 2-(benzo[d]thiazol-2-yl), which was then subjected to use of 5,5-dimethyl-1,3-cyclohexanedione for Michael addition and intramolecular O-cyclization to yield the products [39]. Another synthetic pathway for benzothiazole derivative involves 4 steps initially; thionyl chloride was used to create 4-(chloromethyl) benzoyl chloride (1). Second, a ring closure reaction employing brome solution was used to create derivatives

of 2-aminobenzothiazoles (2a–2b). Thirdly, 2-aminobenzothiazoles (2a–2b) and 4-(chloromethyl) benzoyl chloride (1) reacted to produce four benzo[d]thiazol-2-yl (chloromethyl)-N-(5,6-substituted benzamides (3a–3b). Target compounds (4a–4n) were created in the final step by reacting compounds 3a, 3b with the proper piperazine derivatives. KOH (125 mg, 2.23 mmol) in MeOH (5 mL) solution was mixed with a solution of benzothiazole-2-thiol in MeOH (10 mL) (Hbt, 373 mg, 2.23 mmol). After one hour at normal temperature; the solvent was agitated and totally released from the final yellow solution. After treating the residue with two milliliters of iPrOH, the yellow solid that resulted was filtered and allowed to dry. The production of potassium benzoimidazole-2-thiolate (Kbi) was also accomplished using this process. Graphene oxide (GO) serves as an carbo catalyst that is both effective and recyclable for the environmentally benevolent synthesis of the heterocyclic compound 1,4-benzothiazine from 2-aminothiophenol and a 1,3-dicarbonyl compound. Modern strategies for rapidly assembling complex molecules have been developed as a result of the current utilization of 2-aminobenzothiazole in the multicomponent synthesis of heterocycles [40].

In contrast to traditional techniques, ultrasonication has provided advantages such as increased yields, reduced reaction times, greater selectivity, and less adverse reactions. A novel series of 1,4-disubstituted-1,2,3-triazoles conjugated with fluorinated 1,2,4-triazole–benzothiazole scaffolds can be synthesized through an eco-friendly and efficient ultrasound-assisted methodology, one-pot click cycloaddition method that involves the condensation of sodium azide, 3-(prop-2-ynylthio)-4-alkyl/aryl-5-(2-fluorophenyl), and the appropriate bromoacetamidebenzothiazole.-1,2,4-triazoles 4a-e via a 1,3-dipolar cycloaddition process mediated by Cu(I). Ultrasonic irradiation has various benefits, including the potential to play a significant role in chemistry, particularly in situations where traditional techniques call for high temperatures or lengthy reaction periods. Utilizing non-traditional energy sources, such as microwaves and ultrasonics, may speed up the reaction and lower the likelihood of side product production [41]. Ultrasound on a lab size has surged in prominence in recent years. Ultrasound irradiation has recently become an efficient means of expediting organic reactions.

Compounds like Ethyl 2-(5-substitutedbenzothiazol-2-ylthio)acetate derivatives have been synthesized in yields of 78% and 81% through the reflux of equimolar amounts (0.015 mol) of 5-substituted benzothiazol-2-thiol, ethyl 2-chloroacetate (1.59 g), and potassium carbonate (2.07 g) in acetone for two hours. The solvent was extracted at low pressure when the reaction was finished, and the crude product was subsequently purified via recrystallization from ethanol [42].

At room temperature, organic electrosynthesis provides a clear and concise and bromine-free approach for creating the 2-aminobenzothiazole derivatives. This method employs isopropyl alcohol (i-PrOH) as the solvent and sodium bromide as both the electrolyte and *in situ* brominating agent, enabling the reaction between aniline derivatives and ammonium thiocyanate under mild conditions [43]. We employed a two-step synthesis approach to create 2-benzylsulfonyl benzothiazole derivatives. The first step is a nucleophilic substitution reaction between 2-mercaptobenzothiazole and various benzyl halides (2a-k) to produce the corresponding sulfides. The equivalent sulfones were obtained by oxidizing those sulfides in the second stage.

Methyl-Derivatives of substituted benzothiazoles were created by reacting 3-chloro-4-methoxyaniline when potassium thiocyanate and bromine are present, employing glacial acetic acid as the reaction medium and ammonia as a base catalyst. Using the consize schematic pathway, phenylalanine-containing benzothiazole derivatives were created by treating commercially available benzo[d]thiazol-5-amine (1) with paraformaldehyde, sodium methoxide, and sodium borohydride in methanol to get 2. N-(tert-butoxycarbonyl)-l. The compounds phenylalanine and benzotriazol-1-yl-oxytripyrrolidinophosphonium hexafluorophosphate (PyBOP) in dichloromethane (DCM) and N,N-diisopropylethylamine (DIEA) were then added to 2 to yield 3, and tertiary was then removed [44]. A simple synthetic process was used to create some benzothiazole derivatives. 6-Substituted 2-aminobenzothiazoles were initially synthesized by reacting para-substituted aniline with potassium thiocyanate. This intermediate was subsequently condensed with substituted benzaldehyde and thioglycolic acid when anhydrous zinc chloride is present. In a parallel step, the same substituted benzaldehyde was reacted

with the intermediate in sodium ethoxide to yield compounds bearing identical core structures. Another method for synthesis of benzothiazole Schiff basis is, after dissolving 10 mmol of the benzothiazole derivative (6-Chloro,6-bromo,6-methyl) in 15 mL of 100% ethanol, *o*-vanillin (1.10 g) and a drop of piperidine were added to the mixture. After three hours of refluxing, the mixture was left for eight hours. After filtering and repeatedly washing the yellowish orange solid with cold ethanol, it was dried and recrystallized from carbon tetrachloride to produce a yellow crystalline solid [45].

A catalytic quantity of Fe_3O_4 /collagen (50 mg) was combined with aromatic aldehyde (1.0 mmol) and 2-amino benzothiazole (1.0 mmol) in 4 mL of EtOH, and the mixture was swirled for the designated amounts of time while refluxing.

TLC kept track of the reaction's development. External magnetic fields were used to separate the catalyst, after the reaction was finished, and it was repurposed four times in other new processes with little to no activity loss. EtOH 96% was then used to crystallize the products. Following each run, a magnet was used to extract the catalyst, which was then rinsed with EtOH and dried [46].

The proper arylamine diazonium salts were coupled with 2-(benzo[d]thiazole-2-yl)-3-oxo-pentadinitriles to create a variety of azo benzothiazole derivatives. Pyridazine carbonitrile compounds were also produced by cyclizing azo derivatives with malononitrile in refluxing DMF. Additionally, pyridazine compounds were produced by cyclization of the azo derivatives upon refluxing in DMF [47]. The intermediate 2-hydrazinobenzothiazole (S1) is produced by treating 2-mercapto benzothiazole with hydrazine hydrate. After compound (S1) was treated with phthalic anhydride and two derivatives of pyridazinone and phthalazinone (S3) were produced, resulting in a sequence of compounds (S1–S13). The azomethines (S6–S8) produced by the reaction of (S1) with aromatic aldehyde were further treated with mercaptoacetic acid to yield (S9–S11). There was another 1, 2, 4-triazole (S2) produced when (S1) reacted with *p*-bromophenacyl bromide [48]. Chloroacetic acid and (S1) reacted to produce (S4). When the molecule (S4) reacts with ortho-aminoaniline, benzimidazole (S5) is the end product. A multicomponent process

catalyzed by I₂/DMSO is used to synthesize 2-arylbenzo[d]imidazo[2,1-b]thiazole derivatives. This multicomponent reaction can be conducted under both conventional and microwave heating settings. This methodology's key characteristics include: (i) the creation of one C–C and two C–N bonds in a single pot using metal-free oxidation and cyclization, (ii) the selective synthesis of the fused imidazole ring, (iii) a broad range of substrates, (iv) simple product purification, (v) suitable with many pharmaceutically significant themes, and (vi) the ability to synthesize on a gram scale [49].

Chalcone-amidobenzothiazole conjugate synthesis entails the following steps. The trimethoxy chalcone 4a was synthesized with a favorable yield through the Claisen-Schmidt condensation of isovanilline (6) and trimethoxyacetophenone (5), employing aqueous KOH in ethanol. The (E)-configuration of the synthesized chalcone 4a was predominantly confirmed using this method. Values of the H coupling constant for the proton NMR spectra, when chalcone 4a was etherified with *n*-bromoethyl acetate in dry DMF with K₂CO₃, ester 7 were produced. This ester hydrolyzed with LiOH·H₂O to yield the acid 8, and amide bonds were formed to synthesize conjugates 9a–k using EDCI/HOBt between the acid (8) and many substituted 2-aminobenzothiazoles [38].

Similar to this, 6-aminobenzothiazoles were used to create further analogs. The following is the preparation of the chalcone linked benzo[d]imidazo[2,1-b]thiazole conjugates. Condensing substituted 2-amino-benzothiazoles with ethyl bromopyruvate produced substituted ethyl benzo[d]imidazo[2,1-b]thiazole-2-carboxylate in good yield. These were then reduced with lithium aluminum hydride (LAH) to produce Benzo[d]imidazo[2,1-b]thiazol-2-ylmethanol was substituted, whereby was then oxidized [50]. For duration of three hours at room temperature, a combination of chalcones, nitriles, and ketones of *o*-aminothiophenols was either subsequently refluxed or agitated in a catalytic quantity of concentrated H₂SO₄ in glacial acetic acid. The precipitate that resulted was then filtered, cleaned with water, and allowed to crystallize in the proper solvent. The corresponding 2H-benzo [1, 4]thiazines and 4H-benzo [1] [4]thiazines were produced when *o*-aminothiophenol interacted with ketones which are aromatic and aliphatic that

contained active -hydrogens, respectively. Likewise, in the sync with tricyclic compounds were obtained from the cyclic ketones. Benzo [1] [3] thiazoles were produced by treating o-aminothiophenol with nitriles under the same reaction conditions.

1.3 Rationale of Current Reasearch Work

Numerous benzofused thiazole analogues have been employed as lead compounds in the synthesis and development of medicinal substance, like antiviral, anticancer, anti-inflammatory, and antioxidant ones, according to a study of the literature. Among medications that contain thiazoles are pramipexole, tallpexole, and riluzole. Traditional NSAIDs, including diclofenac, indomethacin, ibuprofen, flurbiprofen, and aspirin, are readily available on the market; however, their use is restricted because of their potential side effects, which include gastrointestinal (GI) hemorrhage, ulceration, addiction, and tolerance, particularly for opiates. The discovery of alternatives to NSAIDs is being attempted all around the world. The mechanism that damages mitochondrial DNA and proteins also involves oxidative stress. Numerous illnesses, including cardiovascular, atherosclerosis, cancer, and inflammation, are brought on by this. The substances that capture free radicals are called antioxidants. The synthesis and development of newly synthesize benzothiazole derivatives as substitute analgesics, anti-inflammatory, and antioxidant agents are the main goal of the current study.

1.4 Aims and Objectives

- a) To synthesize and characterize new derivatives of substituted heterocyclic compounds.
- b) To carry out research utilizing molecular docking and molecular simulation studies on all newly synthesized derivatives.

- c) To perform *in vitro* antioxidant study using DPPH antioxidant assay.
- d) To determine the *in-vivo* anti-inflammatory and analgesic activities of the newly synthesized derivatives.
- e) To conduct acute oral toxicity studies and gross behavioural assessments for all newly synthesized compounds.

Chapter 2

Literature Review

The vast diversity of biological activities and therapeutic uses of benzothiazole derivatives makes them very interesting. Benzothiazole derivatives have demonstrated notable antibacterial activity, as evidenced by reported interactions with a range of biological targets, including dihydroorotase, peptidodeformylase, DNA gyrase, aldose reductase, casdihydrofolatereductase, uridine diphosphate-N-acetyl enolpyruvyl glucosamine reductase (MurB) enoyl-acyl, carrier protein reductase, dehydrosqualene synthase, dihydropteroate synthase, dialkylglycine decarboxylase and tyrosine kinase [51]. Numerous biological actions, including anti-inflammatory, fungicidal, anti-diabetic, analgesic, anti-microbial, antitumor, anti-leishmanial, anti-tumor, anti-rheumatic, and CNS depressant, are exhibited by the BTA scaffold [27]. Certain benzothiazole derivatives have also been utilized to cure analgesia, epilepsy, amyotrophic lateral sclerosis, autoimmune and inflammatory illnesses, and to prevent rejection of solid organ transplants.

2.1 Novel Benzothiazole Based Cytotoxic Agents and Their Mechanisms

Benzothiazole derivatives with selectivity for different anti-tumor receptors have consistently appeared among the altered structures. This comprises substances

that influence the PI3K/Akt/mTOR pathway, interact with receptor tyrosine kinases like C-Met and EGFR, and have antimicrobial properties.

Furthermore, PMX610 [2-(3,4-dimethoxyphenyl)-5-fluorobenzothiazole] and compound 4i have attracted particular interest due to their exceptional anti-tumor activities. As cytotoxic agents, a novel class of benzothiazoles has been created.

The cytotoxic activity of the four benzothiazole derivatives was associated with modulation of free radical production, characterized by an increase in superoxide dismutase activity and a reduction in intracellular levels of reduced glutathione, catalase, and glutathione peroxidase. This imbalance led to elevated levels of hydrogen peroxide, nitric oxide, and other reactive species, ultimately inducing tumor cell death, as evidenced by a marked decrease in protein and nucleic acid synthesis [52].

2.2 Novel Substituted Benzothiazoles as Potent Anti-Inflammatory Candidates

To treat inflammation, a variety of new benzothiazoles have been developed, including 2-(4-butyl-3,5-dimethylpyrazol-1-yl) with 4-butyl-1-(6-substituted-2-benzothiazolyl) benzothiazoles with a 6-substitution. Compounds were demonstrated to have strong anti-inflammatory properties.

When the potential of a new 2-amino-benzothiazole derivative to lower inflammation was examined, it was found that substituting an electron-withdrawing group, such as -Cl, -NO₂, or -OCH₃, at positions 4 or 5 of the 2-amino-benzothiazole greatly enhanced its anti-inflammatory effect.

Furthermore, knowing that it has been discovered that sulphonamides have anti-inflammatory effects, compounds with both sulphonamide and benzothiazole moieties should have a synergistic anti-inflammatory impact [53].

2.3 Benzothiazole Derivatives Emerge as a Strong Pain-Relieving Agent

When the newly synthesized compounds' analgesic properties were screened using Eddy's hot plate method, it was found that compounds with ester, fluoro, and nitrile functional groups in the aliphatic side chain exhibited good analgesic activity; however, when these groups were substituted with NH_2 and OH groups, the analgesic activity decreased.

It was found that the compound with 1, 3-benzothiazole-2-carboxyhydrazide substitution at the 5th position of the oxadiazole ring exhibited extraordinary analgesic activity, when the painkilling activity of 2-(5-substituted-1,3,4-oxadiazole-2-yl)-1,3-benzathiazole derivatives was tested using Eddy's hot plate method [54].

2.4 Mechanistic Insights into Benzothiazole Based Antimicrobial Action

Benzothiazole-based antibacterial compounds exert their effects by binding to various biological targets within bacterial cells and inhibiting key enzymes involved in critical processes such as DNA replication, cell wall synthesis, and cell division or to various biosynthetic pathways of essential bacterial mixtures, including the biosynthesis of histidine and biotin [55]. When benzothiazole derivatives and dihydroorotase interacted molecularly, hydrogen bonds were formed with the active site residues LEU222 or ASN44.

Dihydroorotase inhibition may occur as a result of strong hydrophobic interactions between the bulky thiazole and naphthalene rings at the active site entrance, which may prevent substrates from accessing their binding sites. Therefore, dihydroorotase inhibition may be a factor in these compounds' apparent antimicrobial activities. Regarding reports of their antibacterial and antifungal properties, 2 Marceptobenzothiazoles have been highlighted as strong mechanism-based inhibitors of a

number of enzymes; including acyl coenzyme A, heat shock protein 90, cathepsin D, monoamine oxidase, cholesterol acyltransferase, and c-Jun N-terminal kinases. Using the disc diffusion method, the synthetic compounds' antibacterial activity was assessed. The Agar cup diffusion method was used to investigate the antifungal activity [56].

2.5 Novel Benzothiazole Compounds as a Promising Antidiabetic Agent

Among medicinal chemists worldwide, benzothiazole (BF2) has been one of the most researched moieties for the development of possible antidiabetic medication. In comparison to the common medication acarbose, thiazolidinone-based benzothiazole derivatives exhibit a strong anti-diabetic effect by effectively inhibiting the α -amylase and α -glucosidase enzymes. Regarding this, a number of researches have shown that the agonistic impact of various chemical produced from the benzothiazole nucleus on the peroxisome proliferator-activated receptor gamma (PPAR gamma) is linked to their antidiabetic efficacy. The rate at which L6 myotubes absorb glucose was accelerated by a number of structurally identical benzothiazole derivatives in a manner that was reliant on AMPK. One substance, 2-(benzo[d]thiazol-2-ylmethylthio)-6-ethoxybenzo[d]thiazole (34), increased the rate of glucose absorption by up to 1.1 times when compared to PT-1 and up to 2.5 times in contrast to vehicle-treated cells, so it has strong hypoglycemic activity [57].

2.6 Benzothiazole Derivatives as Versatile Central Nervous System Modulators

Many 2-amino benzothiazole were thoroughly investigated as central muscle relaxants in the 1950s. Several benzothiazole-based drugs have demonstrated exceptional binding affinities to serotonin transporters, 5HT1A, and 5HT2A receptors,

which are crucial sites of action for antidepressant efficacy, in relation to CNS-related pharmacological effects.

Several benzothiazole compounds have demonstrated antidepressant-like properties in a variety of animal models, such as forced swimming tests (FST) and tail suspension tests (TST).

According to bioevaluation tests, substances with 1,2,4-triazole-3-thiol had the greatest anticonvulsant action and good PI among benzothiazole derivatives [25].

The compounds that were examined, 4m N-(6-fluoro-1,3-benzothiazol-2-yl)N-(6-Chloro-1,3-benzothiazol-2-yl) and -2-[5-(pyridin-4-yl)-1,3,4-oxadiazol-2-yl]sulfanylacetamide in both animal models, -2-[5-(pyridin-4-yl)-1,3,4-oxadiazol-2-yl]sulfanyl acetamide prevented seizures at dose levels of 30 mg/kg after 0.5 hours and at 100 mg/kg after 4 hours, suggesting that the compound is strong and have extended-acting time.

2.7 Benzothiazole Analogues Demonstrate Promising Antiepileptic Potential

The antiepileptic activity of numerous benzothiazole analogues, specifically novel thiazolidin-4-one and azetidin-2-one derivatives connected via hydrogen bonding domains, was synthesized and subsequently evaluated.

Comprehensive antiepileptic screening in mice indicated that these synthetic benzothiazole compounds, designated as azetidin-2-one (6a-g) and thiazolidin-4-one (5a-g), possessed good to moderate anticonvulsant efficacy.

It is hypothesized that the observed favorable outcomes are largely due to the strategic placement of electron-withdrawing groups, such as 2,4 -Cl₂ (5c) and 4-NO₂ (5g) on the thiazolidin-4-one's benzene ring at the second position, and 2,4-C₆H₃Cl₂ (6c) on the β -lactam-containing ring [58].

2.8 Phenolic Groups Drive Antioxidant Activity in Novel Benzothiazole Compounds

Notably, a number of investigations have looked into the combination of biological activities, antioxidant properties, and anticancer properties in compounds with sulfur and nitrogen atoms, such as pyrimidines, pyrido-triazolopyrimidines, and tetrahydroisoquinoline-thiones [59]. The phenolic group was revealed to be cause of the antioxidant activity of compounds, revealed that tacrine conjugated phenyl benzo heterocyclic complexes were anti-Alzheimer's agents. Many compounds showed good activity with MIC $\frac{1}{4}$ 0.98–62.5 3 mg/mL and 3.9–62.5 mg/mL, respectively, against the two drug-resistant TB strains, ATCC 35822 and RCMB 2674, when the novel benzothiazole–pyrimidine hybrids were developed and synthesized [60].

2.9 Benzothiazole Compounds Exhibit Remarkable Activity against Influenza A and B Strains

The antiviral activity of the newly synthesized 2-pyrimidylbenzothiazole derivatives was evaluated in vitro against a range of viral strains, including human adenovirus type 7 (HAdV7), coxsackie virus B4 (CBV4), hepatitis A virus (HAV) strain HM175, the ED-43/SG-Feo (VYG) replicon of hepatitis C virus (HCV) genotype 4a, and herpes simplex virus type 1 (HSV-1). Benzothiazole is crucial for the synthesis of antiviral medications, as it comprises a large number of clinically advantageous substances. Fourteen new compounds were evaluated for the development of antiviral medications, and a number of berberine–benzothiazole derivatives were shown to be a novel type of possible agents against influenza virus. The compounds BBD1–BBD14 demonstrated remarkable antiviral properties against influenza A and B virus strains, such as A/PR/8/34, A/Vic/3/75,

B/Lee/40, and B/Maryland/1/59, according to the bioassay results. When oseltamivir was used as a controlled medication in cultured MDCK cells, these compounds shown exceptional antiviral properties [61].

2.10 2-Imidazoliny-Benzothiazoles Show Selective DNA-Binding Activity

Benzimidazole or benzothiazole subunit-containing substituted benzo[b]thieno-2-carboxamides with 2-imidazoliny (the new derivatives) were developed as potentially effective antiproliferative drugs with specific DNA binding capabilities.

It was found that the compounds under test demonstrated moderate to high antiproliferative action against the tested tumor cell lines when substituents were added to the 2-arylbenzothiazole nuclei's C-6 location.

The SAR study indicated that as the incorporation of a hydroxy group to the 2-aryl moiety of the 2-arylbenzothiazole scaffold greatly enhanced susceptibility against tumor cell lines, the addition of substituents to the benzothiazole nuclei benzene ring is necessary for antiproliferative effect [62].

2.11 Novel Benzothiazole-Based Diuretic Agent

Acetazolamide (standard drug) was used in the investigation, and docking analysis revealed that the compound with the most promising diuretic potential was 2-(E)-[(3hydroxyphenyl) methylidene] mino-1,3-benzothi zole-6-sulfonamide.

The Lipinski rule of five, Molsoft for determining molecular features, PASS (prediction of activity spectra for drugs) values for determining the diuretic action, and OSIRIS software for determining toxicity were the five approaches employed to analyse these chemicals [63] .

2.12 2-Amino Benzothiazole Derivatives Protect Against Oxidative Damage

Antioxidants are substances that prevent peroxides from forming, neutralize peroxides, or salvage substances that may produce peroxides. The glial cells produce antioxidant enzymes, which aid in shielding the brain cells from oxidative damage.

The antioxidant effects were assessed using the DPPH and ABTS assays of Schiff's bases made from *o*-Vanillin combined with 2-amino benzothiazole, 2-amino-6-chloro benzothiazole, and 2-amino-6-bromo benzothiazole. While other compounds demonstrated relatively lower activity, all of the compounds shown outstanding effects in the ABTS assay and the DPPH Scavenging Radical assay [64].

2.13 *In Silico* Studies of Benzothiazole Derivatives

One significant stage in the drug development approach is assessing the drug like and central ADMET characteristics of drug candidates. Swiss ADME and pkCSM are two online tools that are used to evaluate these attributes. Swiss ADME is an accommodating online tool that is frequently used to forecast several pharmacological traits for prospective medication candidates.

It contributes significant details about characteristics such drug-likeness, solubility, bioavailability, and lipophilicity. For the sake of preserving time and finances throughout the drug development process, these predictions are essential since they assist in weeding out compounds that might not have good drug like qualities.

In contrast, PkCSM is an online database that concentrates on the key ADMET characteristics of drugs. It aids in evaluating the body's distribution, metabolism, excretion, and absorption of a substance. It also offers details on possible toxic effects, which can assist scientists to detect substances that could be dangerous promptly in the drug development process [65].

Lead compounds can be identified via *In silico* ADME analysis to assess their bioavailability and convenient drug likeness. Clinical trials are missed by over 40% of drug candidates because of poor ADME (absorption, distribution, metabolism, and excretion) characteristics. ADME traits ultimately determine the pharmacological activity and efficacy of medications, which are influenced by drug kinetics and tissue exposure to pharmaceuticals. In one study, 51 benzothiazole derivatives' ADME properties were predicted *In silico* using QikProp [66].

In the early phases of the discovery research process, significant attempts were being made evaluate the similar "drug like" properties of substances in order to forward the discovery and progression of new therapeutics. We have several methods to tackle this problem, but Chris Lipinski and his colleagues at Pfizer came up with the most straightforward and popular one, which is commonly known as the Lipinski Rules. As a general directive, the Rule of Five (ROF) is employed to assess the likeness of drug candidates or to determine if a chemical compound, based on its specific pharmacological or biological activity, exhibits properties indicative of likely oral bioavailability in humans [67].

The process of positioning a ligand or receptor molecule to form a stable complex is known as molecular docking. This orientation is used to forecast binding affinity and the intensity of a ligand-binding interaction and a protein using a scoring algorithm. The drug-receptor interaction predicts a chemical's affinity and activity. Therefore, docking can be used to forecast the nature and potency of the signal. One of the most often used methods in structure based drug design is molecular docking, which can predict how small molecule ligands will bind to the optimal target binding site [68].

According to one of study of molecular docking of benzothiazole derivatives following steps were performed. The protein database provided the urease (PDB ID: 2KAU) and protein (PDB ID: 7EL1) heteromeric structures. In order to prepare the proteins, comparable binding locations, extraneous water molecules, and bond ordering were refined. The 2017 Schrödinger suite's prime module was used to add missing chain atoms. Optimised capability for liquid simulations3 (OPLS3e)

molecular force field with a root mean square difference (RMSD) of crystallographic heavy atoms maintained at 0.3 Å was used to reduce the protein energy. In Schrodinger 2017, substances were molecularly docked with certain proteins [69].

The antituberculosis, antifungal, and anti-inflammatory qualities of the manufactured substance were demonstrated using docking *In silico* studies using Pyrx. The interactions between the investigated drugs and the particular protein targets were ascertained using Pyrx. Cheminfo extracted the smiles from every molecule. Chimera was then used to reduce each structure, and the resulting PDB files were saved. The next stage was to use Open Babel to combine the PDB six structures and turn it into a SDF file that was single. All protein structures were extracted using the RSCB PDB. Chimera was employed to get rid of unnecessary ions, water molecules, ligands, and solvents from all protein structures. In order to compare manufactured substance 5af with the reference molecules, we chose one control molecule per protein target for molecular docking [70].

In order to comprehend the way of binding of newly synthesized benzothiazinones (2af) and their acetate derivatives (3ad), molecular docking experiments were conducted at the molecular level in the VEGFR2 kinase receptor (PDB ID: 6GQO) using Schrödinger 9.6 Maestro edition software. The build panel sketched the ligands in 3D format when they were ready for docking through the use of Lig Prep. The protein for the docking investigation was retrieved from the protein data bank (PDB ID: 6GQO) and synthesized using the protein preparation wizard by adding hydrogen and removing the solvent. Additional minimization was carried out in the presence of bound ligands (F82). Using molecular docking grids made with the co-crystallized bound ligand, the reference ligands (F82) were redocked in the protein catalytic site. This further supported the docking approach by showing that they occupy a similar binding pocket with a root mean square deviation (RMSD) of 0.715 Å. [71]. In order to identify a promising selective BACE1 inhibitor, 96 benzothiazoles were created using the structural characteristics of atabecestat and riluzole. . Atabecestat and compound 72 have BACE-1 docking scores of 7.76 and 7.49, respectively, and corresponding MMGBSA Gbind energies of 70.39 and

68.97 kcal/mol. Atabecestat and compound 72, on the other hand, have BACE2 docking scores of 6.24 and 5.32, respectively, and corresponding MMGBSA Gbind energies of 56.02 and 43.46 kcal/mol.⁸ Using the Schrodinger Maestro³⁷'s build option, the three dimensional structures of all twenty benzothiazole phenyloxadiazole derivatives were sketched. The structure was then further optimized using Ligprep's OPLS 2005 force field, which generated potential tautomers with all possible stereoisomer combinations and the lowest energy conformation. Using Maestro's protein preparation wizard, the human β -D glucuronidase structure (PDB code: 1BHG) 36 was optimized after being retrieved from the PDB database. In order to assign bond order, add hydrogen, add missing disulfide bonds, and remove the B-chain, co-factors, and water molecules, the original crystal structure was pre-processed. A constrained energy minimization was performed with converging heavy atoms to RMSD 0.30 Å, pH 7 was set, and hydrogens of modified species were minimized in order to further improve the structure [72].

Glide, a comprehensive solution for ligand receptor docking in the search for small-molecule drugs suites, was used to conduct docking investigations. The β D glucuronidase's protein structure was first grid generated using receptor grid generation. The middle of the grid box was the catalytic residue Glu540 and provided the β D glucuronidase's x, y, and z coordinates, which were 81.875, 81.601, and 88.010 with a radius of 12 Å, respectively. During the Glide docking process, the standard precision (SP) option was selected, and during analysis, Glide gscore was taken into account. As a docking validation tool, Version 5.1 of GOLD (Genetic Optimization for Ligand Docking) ref. 39) was employed. As a fitness function, the gold scoring function was selected. The genetic algorithm (GA) was chosen because of its 100% search efficiency [73]. .

In order to replicate the way that water molecules and lipid membranes behave in the biological environment, molecular dynamics (MD) simulations use Newton's laws to assess the motions of water, ions, small molecules, macromolecules, and more complex systems, such as entire viruses. To study the recognition pattern of ligand protein or protein-protein complexes, structural motions such as those that depend on temperature and solute/solvent are particularly crucial. In this

regard, MD simulations are very helpful because, this methodology can be employed for modeling these motions. [74]. The physical motions and dynamic of the (Comp.16LU7) and (Comp.16 M18) complexes were investigated using MD simulations. The Schrödinger's Desmond package was used to execute the MD simulation in accordance with a previously documented protocol. In order to assess the Complex stability is estimated by RMSD values; lower RMSD values indicate better stability), ligand protein for 100 ns, complexes was simulated. For SARSCoV2 Mpro and ACE2, the protein RMSD trajectory varied for up to 5 and 15 ns, respectively, before steadily stabilizing. There was minimal variation during the 100 ns simulation for the (Comp.16LU7) complex, indicating a higher level of stability. At equilibrium, Mpro (6LU7) and ACE2 (6 M18) had respective RMSD average values of 1.8 and 9.5 Å (Fig. 4). It is acceptable for tiny globular proteins to have a variation of 1-3 Å [75]. To perform a comparative study, the compounds with the greatest docking scores were selected, and accepted benchmark substance. All complexes had average RMSDs between 2.05 and 3.05 Å, which suggests that the molecules were highly stable during the MD simulation. The Lck-benzothiazole complexes were stable for the duration of the MD simulation, according to the RMSD analysis. The durability of these complexes was further corroborated by the RMSF graphs, which showed that the N-terminal area fluctuated more (6.0 Å) than the C terminal region (2.5 Å). Maintaining the structural integrity of the molecule receptor contact depends on the C terminal portion of the complex remaining more stiff and stable, as indicated by the reduced fluctuation there. Throughout the simulation, we also kept an eye on the ligands' no bonded interactions, which provide light on how they engage with the receptor and hold their locations while enhancing stability [66]. The calculation of interaction energy provides insight into the binding strength between the ligand and the target protein. To validate the binding affinities obtained from molecular docking studies, a thorough analysis of free energy of interaction between the ligands and protein structures was performed. Receptor and ligand hydrogen bonding is essential for the robustness of the ligand-protein complex; it is also necessary for drug selectivity, metabolism, and adsorption. this analysis shows the total number of hydrogen bonds formed during MD simulation [76].

Chapter 3

Materials and Methods

3.1 Materials and Methods

3.1.1 Chemicals and Solvent

The synthesis had employed chemicals and solvents such as Triethanolamine (TEA), 1-Chloroacetylchloride, 2-Aminobenzothiazole, Dichloromethane (DCM), Sodium bicarbonate, Dimethylformide (DMF), ethylacetate, petroleum ether, ethanol, methanol, and other reagents.

3.1.2 Software's for *In silico* Studies

Software tools including ChemBioDraw, PyRx, Schrodinger's MD simulation and Auto Dock was utilized for molecular docking & simulation studies.

3.2 Methodology

3.2.1 Experimental

Synthesis involved 2 step reactions.

3.2.1.1 *General Scheme for the Synthesis of 2,2-chloroacetoaminobenzothiazole (F1)*

Monochloroacetyl chloride and aminobenzothiazole were reacted in equimolar proportions in a round-bottom flask under continuous stirring at 300 RPM, with the reaction temperature maintained between 0°C and 25°C. Triethylamine (TEA) was added as a catalytic base, and the reaction was permitted to continue overnight. On the next day, the reaction blend was quenched with ice, allowed to reach room temperature, and subsequently filtered to isolate the final product (F1) in powdered form [31].

Following main steps were involved; 1) In round bottom flask, DCM solvent (10-15ml) was added and then 2-Aminobenzothiazole (320mg) was added and placed on magnetic stirrer, to dissolve it completely. 2) After dissolving the above solution completely, Triethanolamine (TEA) (300microlitre) was added drop wise with continuous stirring. 3) Monochloroacetylchloride (66.2 micro liter) was added drop wise to above solution on ice bath in order to maintain the temperature condition at 0-5°C as the Monochloroacetylchloride could result in highly exothermic reaction at higher temperature. 4) Reaction mixture was then stirred for 24 hours at room temperature (0-25°C) and product was obtained in crystalline powder form after filtration and purification.

Colourless powder; Yield 85%; melting point 184 °C. IR (cm⁻¹): 3100 (N-H), 3055 (Ar-C-H), 2900 (Alkyl C-H), 1485 (Ar-C=C). ¹H NMR (400 MHz, CDCl₃): δ 4.25 ppm (CH₂, s), 7.2-7.8 ppm (Ar-H, m). ¹³C NMR (100 MHz, CDCl₃): δ 160 ppm (C-2), 120-126 ppm (C4-C9), 164 ppm (C11), 42.25 ppm (C13). Elemental analysis: C (47.69%), H (3.11%), N (12.36%), O (7.06%), S (14.15%).

3.2.1.2 *General Scheme for Synthesis of N,N'-bis[(2,3-dihydro-1,3-benzothiazol-2-yl)] (F2)*

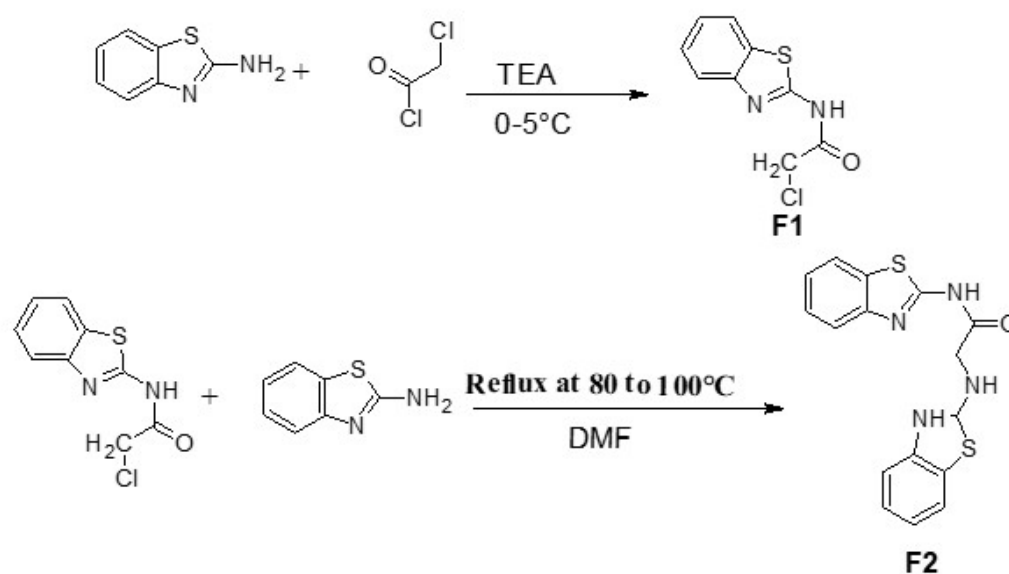
In the second step the product of first reaction *2,2-chloroacetoaminobenzothiazole* was reacted with 2-Amino benzothiazole in presence of base sodium bicarbonate

at 80°C. under reflux conditions. Following steps were involved in synthesis;

1) 2,2-chloroacetoaminobenzothiazole (10mg) was dissolved in DMF (10-15ml) in round bottom flask with continuous stirring on magnetic stirrer. 2) 2-Aminobenzothiazole (20mg) was added to above mixed solution at temperature 0-25 °C with continuous stirring.

3) Sodium Bicarbonate (12.77mg) was added as base to mixed solution in round bottom flask. 4) Reaction mixture was then heated at 80 °C under reflux conditions for 24 hours. 5) Final product was obtained in white crystalline form by evaporating solvent through rotary evaporator, and then purification was performed.

Colourless powder; Yield 88%; melting point 184°C; IR cm^{-1} ; 3300 cm^{-1} (N-H), 1670 cm^{-1} (C=O) , 1485 cm^{-1} (Ar-C=C), 3055 cm^{-1} (Ar-C-H), 2900 cm^{-1} (Alkyl C-H) , ^1H NMR: δ 8.82ppm (CH₂, Singlet), δ 11.15 ppm (CH, Singlet), δ 5.9-7.8ppm (Ar-H, Multiplets), ^{13}C NMR:149.05ppm (C2), 116.01-116.38ppm (C4-C9), 161.55ppm (C11), 29.77ppm (C13), 108.11ppm (C15), 127.20-127.5ppm (C17-19), C(56.12%) H(4.12%) N(16.36%) O(4.67%) S(18.73%)



Scheme 1: General Scheme for Synthesis of Benzothiazole derivatives

3.2.2 *In Silico* Studies

3.2.2.1 *ADMET Properties of Synthesized Compounds*

One significant stage in the drug development approach is assessing the drug like and central ADMET characteristics of drug candidates. Swiss ADME and pkCSM are two online tools that we used to evaluate these attributes.

Swiss ADME is an accommodating online tool that is frequently used to forecast several pharmacological traits for prospective medication candidates. It contributes significant details about characteristics such drug-likeness, solubility, bioavailability, and lipophilicity. ADMET properties of compounds F1 and F2 was analysed by SWISS ADME online freeware [77].

3.2.2.2 *Molecular Docking Studies*

3.2.2.2.1 *Retrieval of receptors structure from Protein Data Bank*

The three-dimensional (3D) structure of the receptor was retrieved from the Protein Data Bank (PDB) (<https://www.rcsb.org>) using the PDB ID as mentioned as the name COX-2, PDB ID 3 LNI and organisms *Mus Musculus*. Preparation of the target proteins for molecular docking was carried out using AutoDock Tools, which involved optimization of the protein structures and assignment of appropriate charges and atom types. Energy minimization was performed, Gasteiger charges were assigned, and the structures were saved in PDBQT format. Hydrophobicity profiles and Ramachandran plots were generated using Discovery Studio 4.1 Client (2012). Additionally, the secondary structural features—such as helices, β -sheets, coils, and turns—along with their respective statistical distributions, were analyzed using VADAR version 1.8. [78].

3.2.2.2.2 *Ligands-Molecular Docking* The Ligands were intrigued in ChemBioDraw Ultra and preserved in PDB format using Discovery Studio client 4.0 after energy minimization. Ligand structures were prepared using AutoDock

Tools in their most stable conformations. Kolaman & Gasteiger charges were assigned, and the ligands were kept in PDBQT format.

Molecular-docking studies were then performed using PyRx, targeting all synthesized ligands against the insulin receptor and guanylyl cyclase receptor [78] virtual screening was conducted using the AutoDock Vina Wizard approach, enabling efficient docking of the synthesized ligands to the active sites of the target receptors [79].

The grid box center values for COX-2 (PDBID: 3LN1) were set at centre X = 35.862, centre Y = -27.493, center Z = -10.188 and size values were adjusted as X = 67, Y = 73, and Z = 77 and size metrics were modified to ensure optimal conformational positioning within the active site of each target protein, ligands were docked by itself opposed all selected receptors using a 50 as the default exhaustiveness value.

The resulting docked complexes were assessed based on their lowest values of binding energy (kcal/mol), which served as a measure of binding affinity. The Discovery Studio Visualizer was used to create Three-dimensional graphical representations of the docked complexes. (Version 4.0, 2012).

3.2.2.2.3 Structural analysis of target proteins The structural analysis of the target protein COX-2 revealed that it comprises approximately 42% α -helices (829 residues), 8% β -sheets (161 residues), 49% random coils (1011 residues), and 5% turns (126 residues), totaling 2207 amino acid residues. The crystallographic R-value of the selected structure was 0.231, with a resolution of 2.3 Å.

The unit cell parameters were determined as a = 180.95 Å, b = 135.38 Å, and c = 124.08 Å, with α , β , and γ angles each measured at 90°. Structural validation through the Ramachandran plot indicated that 98% of the residues occupied the permitted territories of the ϕ (phi) and ψ (psi) dihedral angles, confirming the reliability of the protein model. A detailed representation of the Ramachandran plot is provided in Figure 3.1.

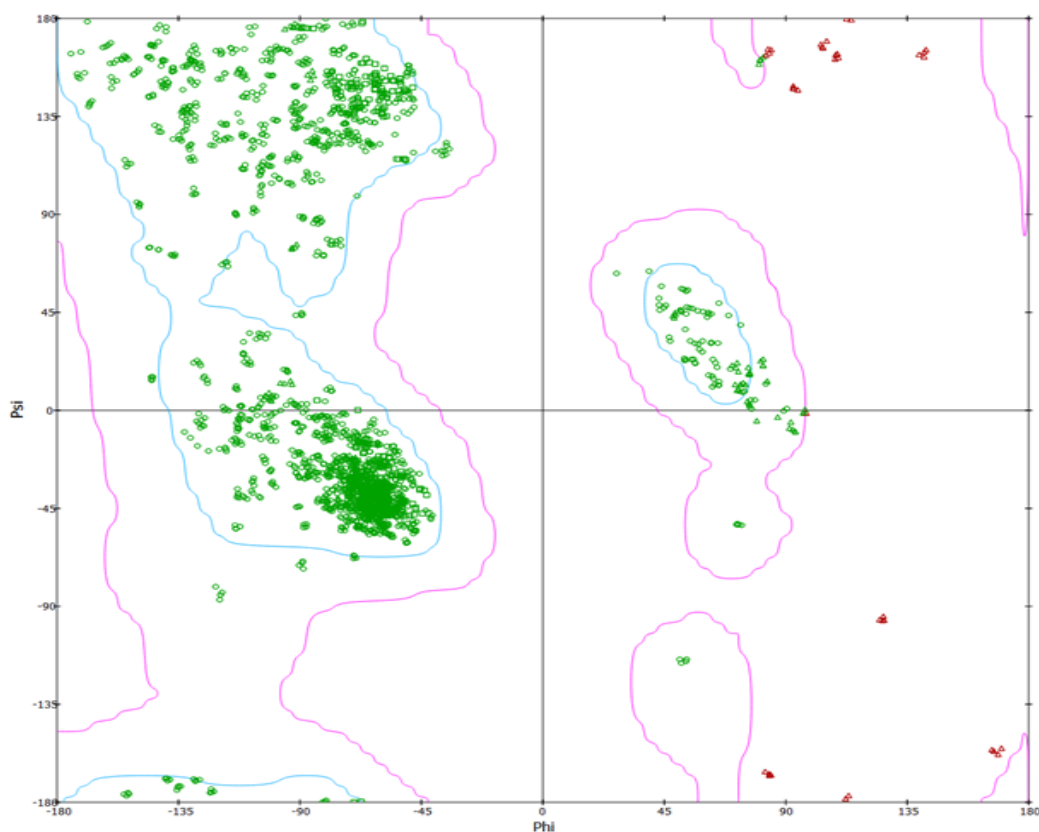


FIGURE 3.1: RAMACHANDRAN plots for COX-2 (PDB ID: 3LN1).

3.2.2.3 *Molecular Dynamic Simulation*

Simulation molecular dynamic of protein-ligand complex were performed using software (desmond-md-job-F2-5kIR). The complex was solvated in an orthorhombic box containing the TIP3P water model, and the system's charge was neutralized by adding Na^+ and Cl ions. The simulation box volume was reduced by 50%. Subsequently, the root-mean-square deviation (RMSD) was calculated regarding each orientation to assess simulation stability [80].

3.2.2.4 *Chemoinformatic Properties*

Molinspiration and ChemBioDraw are widely used chemoinformatics tools employed to evaluate key molecular properties and assess drug-likeness of synthesized compounds. These software platforms enable researchers to calculate critical physicochemical descriptors, predict bioactivity, and analyze compliance with

Lipinski's Rule of Five (Ro5) – a crucial set of guidelines that helps predict a compound's potential as an orally active drug.

3.2.3 Pharmacological Evaluation

To determine their biological efficacy, particularly their analgesic and anti-inflammatory properties, the synthesized compounds had be served with exposure to screening tests. Additionally, the compounds had undergo safety evaluation through acute oral toxicity studies.

3.2.3.1 *In-vitro* Assays

3.2.3.1.1 Antioxidant Potential Evaluation Using DPPH Assay The free radical scavenging potential of compound F1 & F2 was evaluated using ascorbic acid and the DPPH test, where ascorbic acid serve as the positive control. Serial dilutions of F1 & F2 (1-1000 $\mu\text{g}/\text{mL}$ in DMSO/Tween-80) were mixed with methanolic DPPH solution (1 mM) and incubated in dark for 30-45 minutes. The reduction of purple DPPH to yellow indicated antioxidant activity, measured spectrophotometrically at 517 nm, and expressed as percentage antioxidant activity using the formula:

$$\text{PSA} = \frac{(\text{Absorbance of control} - \text{Absorbance of sample}) \times 100}{\text{Absorbance of control}}$$

Percentage scavenging activity (PSA) was calculated from triplicate experiments and results were averaged [81]. IC_{50} values were determined using Graph Pad Prism.

3.2.3.2 *In-vivo* Assays

3.2.3.2.1 Induction of Carragenan Triggered Inflammatory Pain and Thermal Hyperalgesia Study Thermal hyperalgesia was evaluated using a

hot plate assay. Mice (n=4/group) were individually placed in a plexiglass chamber on a hot plate maintained at 55°C. The latency to paw withdrawal (licking, flicking, or jumping) was recorded with a stopwatch as a nociceptive response. Mice were divided into four groups (n=4/group). First Group was of negative control group that was given no drug; only pain was induced using carrageenan. Second group comprises positive control to which the standard drug (Diclofenac) was given at dose of 3mg/kg at one hour prior to induction of pain. Third group was of treatment group to which the drug F1 was given dose 10mg/kg. Fourth group was given test drug F2 was given dose 10mg/kg. All mice were acclimatized to testing environment temperature on hot plate chamber. Treatment groups were placed on Hot plate 30 minutes after administration of specified drugs. Mice were placed on Hot plate one by one, time was noted on hot plate of mice paw withdrawal movements. Time was noted for negative control group, treatment groups and positive control group after 5, 10 and 15 seconds. Comparison was made between groups and readings noted were plotted on graph pad prism. To avoid tissue injury, a cut off time of 30 seconds was enforced [82].

3.2.3.2.2 Anti-Inflammatory Evaluation of Synthesized Benzothiazole Derivative The anti-inflammatory effects of the synthesized compounds were evaluated using a carrageenan-induced paw edema assay in mice. Diclofenac (3mg/kg) served as the positive control. F1 and F2 were dissolved in a vehicle of 3% DMSO + 1.5% Tween-80 and administered intraperitoneally (5 mL/kg) to randomized mouse groups (n=4/group) at a 10 mg/kg dosage. The vehicle was given to control group alone. Thirty minutes post-administration, acute inflammation was induced by injecting carrageenan (100 μ L) in the right hind paw. Volume of the paw was measured (pre-carrageenan) at 3 hours post-carrageenan injection to quantify edema formation [54].

3.2.3.2.3 Acute Oral Toxicity Profiling The acute oral toxicity of synthesized compound F1 and F2 were evaluated following OECD guidelines using healthy male albino mice (34 ± 10 g). Mice were divided into four groups (n=4):

Group A (control, 0.9% saline), Group B (DMSO 5%) Group C (F1 100 mg + DMSO5%) and Group D (F2 100 mg + DMSO5%). No lethal dose (LD_{50}) was observed, so the maximum tolerance dose (MTD) was assessed. Animals were housed under standard conditions ($25 \pm 2^{\circ}\text{C}$, $65 \pm 5\%$ humidity, 12 h light/dark cycle) with free availability to diet and water. Behavioural monitoring was conducted for 14 days, after which mice were euthanized via cervical dislocation. To facilitate histopathological assessment (H&E staining), key organs such as the heart, liver, spleen, kidneys, stomach, and lungs were removed [83].

Chapter 4

Results and Discussion

4.1 Results and Discussion

4.1.1 Experimental

The compounds F1 and F2 were synthesized according to the reported method. The synthesis involved a two-step reaction to produce *N,N'*-bis[(2,3 - dihydro - 1,3 - benzothiazol - 2 - yl)](F2). In the first step, *2,2-chloroacetoamnbenzothiazole* (F1) was synthesized by reacting monochloroacetyl chloride with 2-aminobenzothiazole in dichloromethane (DCM) at 0–25 °C, using triethylamine (TEA) as a catalyst. The reaction was stirred for 24 hours, followed by ice quenching, filtration, and purification to yield the product as a crystalline powder [31].

In the second step, F1 was further reacted with 2-aminobenzothiazole in DMF in the presence of sodium bicarbonate as a base. The mixture was refluxed at 80 °C for 24 hours, after which the solvent was evaporated, and the final product (F2) was obtained as white crystals upon purification. The process ensured controlled exothermic conditions and efficient product isolation through filtration and solvent removal. The final products were purified through multiple rounds of column chromatography, and their purity was confirmed by thin-layer chromatography

(TLC) and elemental analysis [32]. Both compounds were obtained in good yields. Structural confirmation was achieved using ^1H NMR and ^{13}C NMR spectroscopy, which validated the successful synthesis and purification of F1 and F2.

Multiple successive rounds of column chromatography were employed to purify and isolate the final compounds. Purity of all the compounds was confirmed with the help of TLC. All the products were obtained in good yields. FT-IR, ^{13}C NMR and ^1H NMR spectroscopic data further confirmed the structures of final compound F1 & F2 and their purification.

TABLE 4.1: FT-IR ($\bar{\nu}$ (cm^{-1})) spectral data of F1 and F2 compounds.

Compound	N-H	C=O	N-H	C=C
	Stretch	Amide	Bend	Aromatic
F1	3100	–	1650	1485
F2	3300	1670	1650	1485

Infrared (IR) spectroscopy confirmed characteristic functional groups, including an N-H stretch at 3100 cm^{-1} , aromatic C=C vibrations at 1485 cm^{-1} , and alkyl C-H stretches at 2900 cm^{-1} . IR analysis revealed an N-H stretch at 3300 cm^{-1} and a strong C=O absorption at 1670 cm^{-1} , consistent with the amide linkage as shown in figure 4.1.

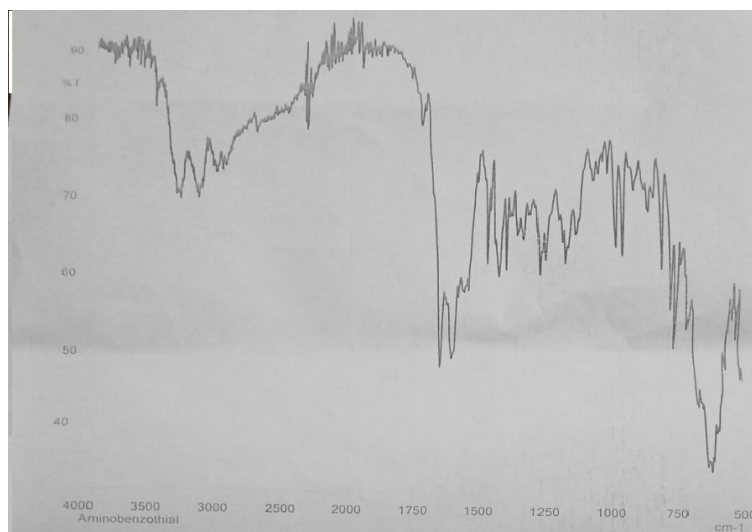
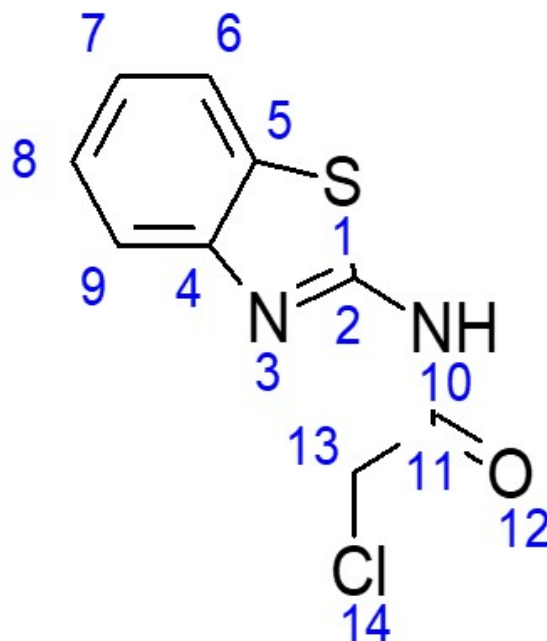


FIGURE 4.1: FTIR Results of F2 Compound

4.1.2 ^1H NMR (δ , ppm) and ^{13}C NMR (δ , ppm) spectral data of F1



S.N	Proton Numbers	Chemical Shift (δ -ppm)	Multiplicity
01	2H	4.25	S
02	4H	7.2-7.8	M

The synthesis of N-(1,3-benzothiazol-2-yl)-2-chloroacetamide (F1) yielded a colorless powder with a melting point of 184 °C, obtained in 85% yield. The ^1H NMR spectrum exhibited a singlet at δ 4.25 ppm corresponding to the chloroacetyl $-\text{CH}_2-$ protons, while aromatic protons appeared as multiplets between δ 7.2–7.8 ppm.

S.N	Chemical Shift (-ppm)	Carbons
01	160	C-2
02	120-126	C4-C9
03	164	C11
04	42.25	C13

^{13}C NMR analysis further supported the structure, with key signals at 160 ppm (C-2 of benzothiazole), 164 ppm (amide carbonyl, C11), and 42.25 ppm (chloroacetyl carbon, C13). Elemental analysis aligned well with the theoretical composition (C, 47.69%; H, 3.11%; Cl, 15.64%; N, 12.36%; O, 7.06%; S, 14.15%), confirming purity.

4.1.3 ^1H NMR (δ , ppm) and ^{13}C NMR (δ , ppm) spectral data of F2

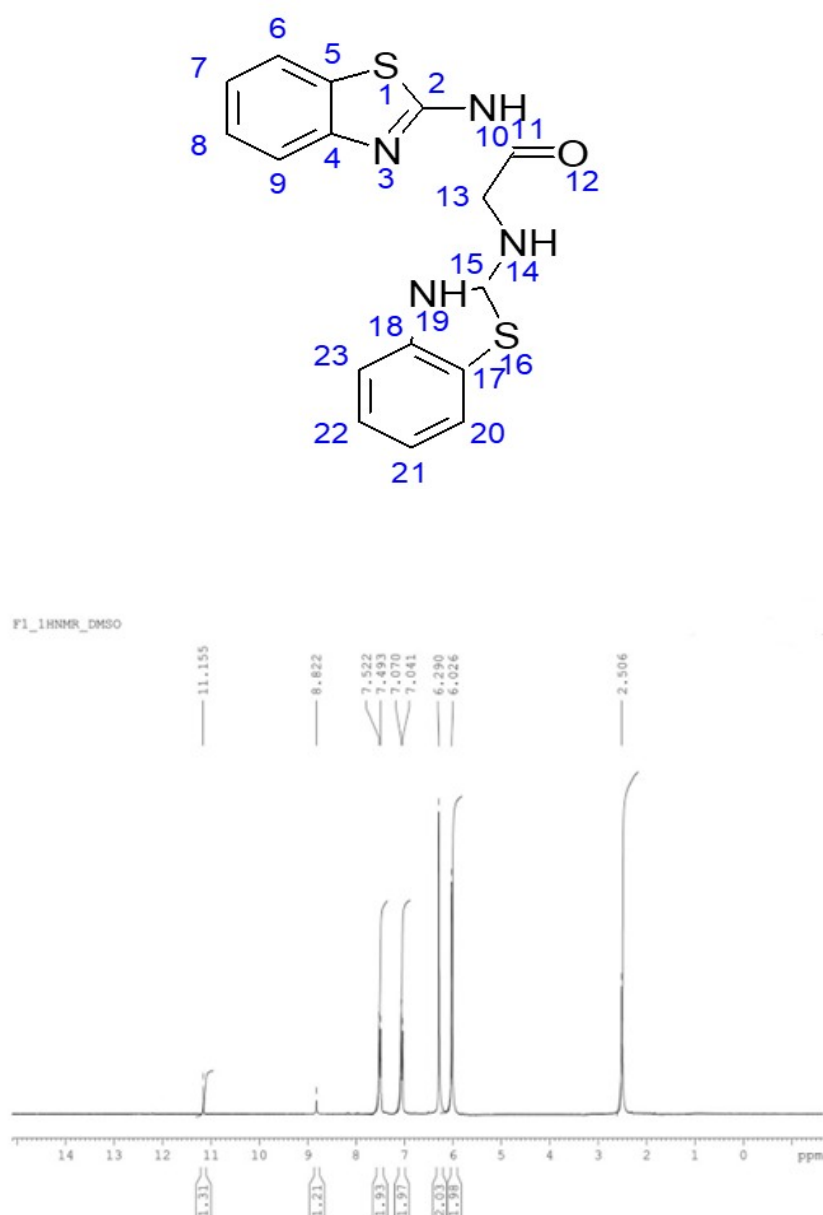


FIGURE 4.2: ^1H NMR (δ , ppm) of Compound F2

S.N	Protons	Chemical Shift (-ppm)	Multiplicity and Coupling Constant
01	2H	8.82	S
02	1H	11.15	S
03	8H	5.9-7.8	M

The subsequent reaction yielded N-(1,3-benzothiazol-2-yl)-2-[(2,3-dihydro-1,3-benzothiazol-2-yl)amino] acetamide F₂, also as a colorless powder with a 88% yield and a melting point of 184 °C. The ¹H NMR spectrum displayed a singlet at δ 8.82 ppm for the -CH₂ group and a broad singlet at δ 11.15 ppm for the NH proton, while aromatic protons resonated between δ 5.9–7.8 ppm as shown in figure 4.2.

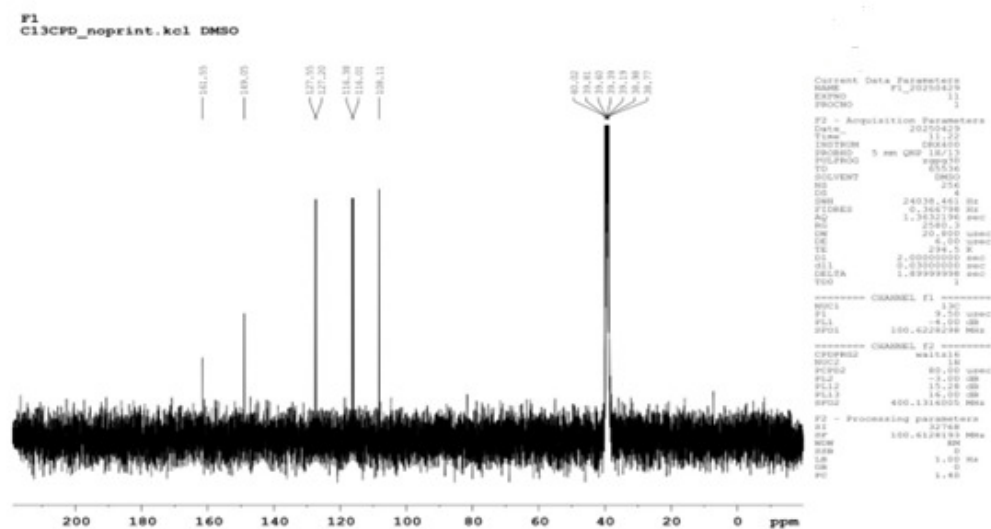


FIGURE 4.3: ¹³C NMR (δ ppm) of Compound F2

S.N	Chemical Shift (δ -ppm)	Carbon
01	149.05	C2
02	116.01-116.38	C4-C9
03	161.55	C11
04	29.77	C13
05	108.11	C15
06	127.20-127.55	C17-19

^{13}C NMR data confirmed the structure, with signals at 149.05 ppm (C2), 161.55 ppm (amide carbonyl, C11), and 108.11 ppm (C15, urea-like carbon) as shown in figure 4.3. Elemental analysis (C, 56.12%; H, 4.12%; N, 16.36%; O, 4.67%; S, 18.73%) matched the expected composition, validating the successful synthesis and purification of F2. The spectroscopic and analytical data collectively confirmed the structural integrity and high purity of both compounds.

4.1.4 Physical data of synthesized compounds

The synthesized compounds F1 and F2 were purified by column chromatography obtained as a colourless powder. Melting points ranged from 180-185 °C. The percentage yield of the compounds was 85% and 88%, respectively. The compounds additionally fulfilled the criteria for the Lipinski rule of five. Detailed physical properties and chemo-informatics properties are given in Table 4.2.

TABLE 4.2: Physical properties of F1 and F2

Property	F1	F2
Molecular Formula	$\text{C}_9\text{H}_7\text{ClN}_2\text{OS}$	$\text{C}_{15}\text{H}_{14}\text{N}_4\text{OS}_2$
Yield	85%	88%
Color	Colorless (Solid)	Colorless (Solid)
Formula Weight	226.68268	330.42786
Composition	C(47.69%) H(3.11%) Cl(15.64%) N(12.36%) O(7.06%) S(14.15%)	C(54.52%) H(4.27%) N(16.96%) O(4.84%) S(19.41%)
Molar Refractivity	$59.69 \pm 0.3 \text{ cm}^3$	$91.96 \pm 0.4 \text{ cm}^3$
Molar Volume	$150.7 \pm 3.0 \text{ cm}^3$	$217.7 \pm 5.0 \text{ cm}^3$
Parachor	$430.5 \pm 4.0 \text{ cm}^3$	$654.0 \pm 6.0 \text{ cm}^3$
Index of Refraction	1.722 ± 0.02	1.786 ± 0.03
Surface Tension	$66.6 \pm 3.0 \text{ dyne/cm}$	$81.3 \pm 5.0 \text{ dyne/cm}$
Density	$1.504 \pm 0.06 \text{ g/cm}^3$	$1.51 \pm 0.1 \text{ g/cm}^3$
Dielectric Constant	Not available	Not available
Polarizability	$23.66 \pm 0.5 \times 10^{-24}$	$36.45 \pm 0.5 \times 10^{-24}$
RDBe	cm^3 7	cm^3 11
Monoisotopic Mass	225.996761 Da	330.060901 Da
Nominal Mass	226 Da	330 Da
Average Mass	226.6827 Da	330.4279 Da

4.2 *In Silico* Studies

4.2.1 *ADMET* Properties

TABLE 4.3: ADMET Properties of synthesized compounds (F1 and F2)

S.N	ADMET	Comments	F-1	F-2
01	Absorption			
	Water solubility	Low aqueous solubility	-5.78 to 3.34.	-5.78 to 3.34.
	Caco-2 Permeability	Variable intestinal permeability	-1.46 to 1.57	-1.46 to 1.57
	Human intestinal Absorption	High absorption rates anticipated in Humans.	90% to 95%	90% to 95%
02	Distribution			
	Blood Brain Barrier Permeability	Moderate to low potential for bridging the BBB	-0.21 to 0.24	-0.21 to 0.24
03	Metabolism			
	Cytochrome P450 Interactions:	No sufficient knowledge available	Interacted with Cyp3A Enzyme	Interacted with Cyp3A Enzyme
04	Excretion			
	Total Clearance	Modest excretion rates.	0.85 to 0.96 mL/min/kg	0.85 to 0.96 mL/min/kg
05	Toxicity			
	AMES Toxicity	Mutagenic qualities.	Positive	Positive
06	Hepatotoxicity	Divergent prediction	Hepatotoxic ramification	Hepatotoxic ramification

The Absorption, Distribution, Metabolism, Excretion and Toxicity (ADMET) analysis of compounds F1 and F2 reveals key pharmacokinetic and safety profiles. Both compounds exhibit low aqueous solubility (-5.78 to -3.34) but demonstrate high human intestinal absorption (90–95%), suggesting effective oral bioavailability despite solubility challenges. Caco-2 permeability varies (-1.46 to 1.57), indicating moderate intestinal absorption variability as depicted in Table 4.3.

Distributionally, both show moderate-to-low blood-brain barrier (BBB) penetration (-0.21 to 0.24), reducing CNS-related side effects. Metabolically, they interact with CYP3A4, necessitating caution in drug-drug interactions.

Excretion rates are modest (0.85–0.96 mL/min/kg), while toxicity assessments raise concerns: both compounds show mutagenic potential (AMES-positive) and hepatotoxic ramifications, highlighting the need for further structural optimization to mitigate toxicity risks.

Overall, while F1 and F2 possess favorable absorption and distribution traits, their metabolic interactions and toxicity profiles warrant careful evaluation in preclinical development.

4.2.2 Molecular Docking Studies

Molecular docking studies were conducted to evaluate the binding affinity between the target proteins and the synthesized ligands.

TABLE 4.4: Highest binding affinity of F1, F2, and Diclofenac with COX-2 (PDB ID:3LN1)

Name	PDB ID	Lowest Binding energy kcal/mol with F1	Lowest Binding energy kcal/mol with F2	Lowest Binding energy with CLOFENIC
COX-2	3LN1	-6.8	-7.5	-8.0

Docking simulations were carried out using the AutoDock Vina engine [79] integrated within the PyRx user interface [84]. The binding energy values (expressed in kcal/mol) were employed to estimate the strength of interaction and to identify the most favorable docking poses. These values provided insight into the predicted binding free energy and the corresponding binding constants of the ligand–protein complexes, as summarized in Table 4.4.

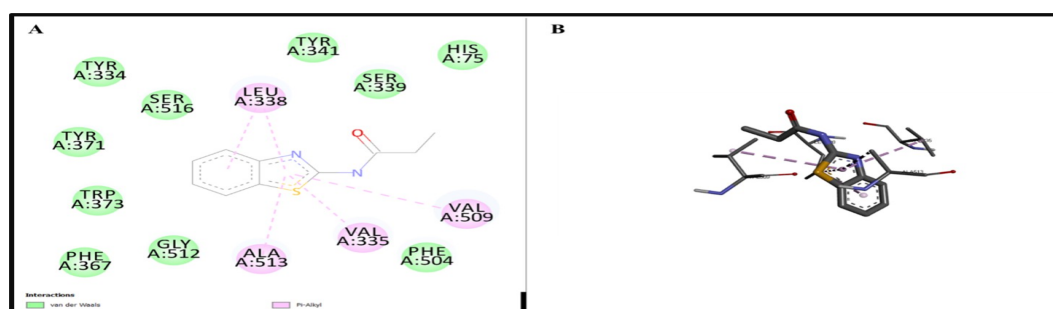


FIGURE 4.4: 2D and 3D presentation of binding interactions of F1 with the binding site of COX-2 (PDB ID: 3LN1)

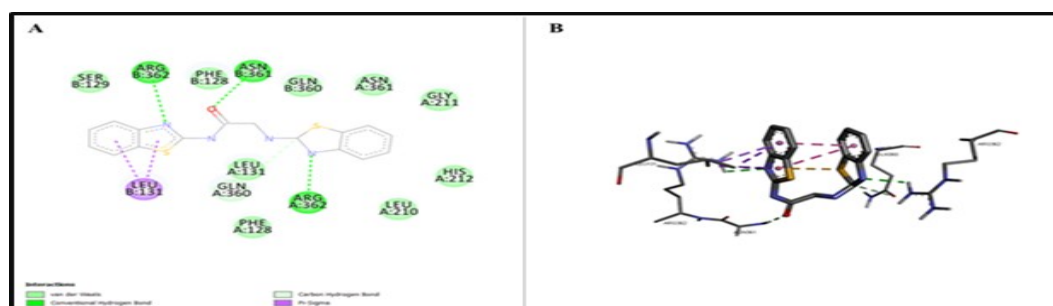


FIGURE 4.5: 2D and 3D presentation of binding interactions of F2 with binding site of COX-2 (PDB ID: 3LN1).

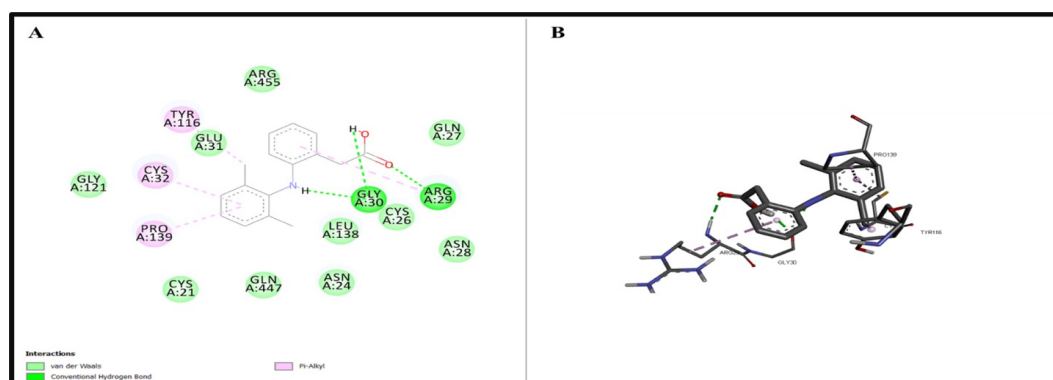


FIGURE 4.6: 2D and 3D presentation of binding interactions of Diclofenac with binding site of COX-2 (PDB ID: 3LN1)

Molecular docking analyses were undertaken to determine the binding interactions between the synthesized ligands (F1 and F2) and the selected protein targets. The docking simulations were performed using AutoDock Vina integrated into the PyRx interface, with binding affinities expressed in free energy values (kcal/mol) [85]. The results indicated that both compounds exhibited notable binding affinities, with F2 showing a higher affinity (-7.5 kcal/mol) toward COX-2 (PDB ID: 3LN1) compared to F1 (-6.8 kcal/mol). For reference, the standard drug diclofenac demonstrated a binding affinity of -8.0 kcal/mol with the same target. These findings suggest that F2 may possess significant inhibitory potential against COX-2, warranting further investigation into its therapeutic applications.

Results of 2D and 3D Diagram of molecular docking analysis showed that as in figure 4.4, F1 compound had Van der waal type of bonding to the amino acid residues like Tyr:A341, Trp A:371, Gly A:512, His A:75 and TRPA:373, and Pi-Alkyl type of bonding to LEUA:341, ALAA:513, VALA:335 and VALA:509 residues to the core of rings. figure 4.5 showed that compound F2 had van der waal bonding to amino acid residues PHEB:128, GLNB:360, ASNA:361, Conventional Hydrogen bonding to Arg B:362, Asn B:361 and Arg A:362 to oxygen and nitrogen atoms, Carbon Hydrogen bonding to GLNA:360, and Pi-Sigma bonding to LEUB:131. figure 4.6 demonstrated that Diclofenac had Van der waal bonding to residues Glu A:31, Gly A:121 and Gln A:27, conventional hydrogen bonding to GLYA:3 and ARG A:29 to the hydrogen and oxygen atoms and Pi-Alkyl bonding to TYRA:116, PROA:139 and CYSA:21 to core of rings so it was concluded that F2 had shown more strong binding affinities to the Protein amino acid residues.

4.2.3 Molecular Dynamic Simulation

4.2.3.1 RMSD Analysis

As a quantitative measure, the Root Mean Square Deviation (RMSD) indicates the average difference in atomic positions for a selected group of atoms in a specific trajectory frame against a predefined reference frame.

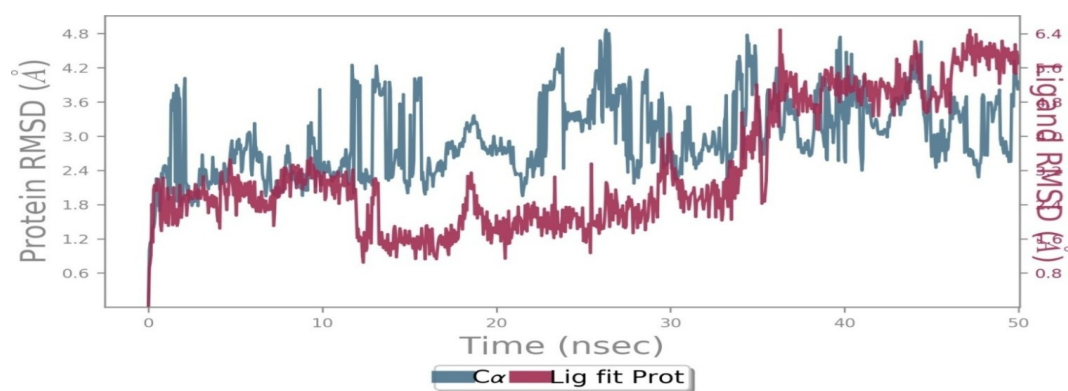


FIGURE 4.7: RMSD Analysis of F2 Compound with target protein

Figure. 4.7 showed that average RMSD for the protein was found to be 1.3Å (blue). There was a slight variation between 12 and 30 s stabilizing at approximately 33 ns after achieving equilibrium. The average RMSD for Ligand RMSD was 5.0Å (red). A similar fluctuation pattern was seen across 46 to 49 ns, stabilized at 50 ns, and remained steady over the simulation throughput. Monitoring the root-mean-square deviation (RMSD) of a protein throughout a molecular dynamics simulation provides valuable insight into its structural stability and conformational behavior.

As the simulation progresses, the RMSD typically fluctuate around a thermally averaged structure and stabilization of these fluctuations indicates convergence. For small, globular proteins, RMSD deviations in the range of approximately 1–3 Å are generally considered acceptable. In contrast, larger deviations may reflect significant conformational changes occurring during the simulation. Stabilization of RMSD values around a consistent average is essential to confirm the system has equilibrated.

Conversely, if the RMSD continues to rise or decline toward to the simulation's closing, it may suggest that equilibrium has not been accomplished and that the simulation duration may be insufficient for reliable structural evaluation. The cohesiveness associated with the ligand within the protein's interacting site during the simulation is shown by the ligand RMSD, which is shown on the right Y-axis. Following the alignment of the protein ligand complex on the protein pillar of the reference and the evaluation of the heavy atoms in the ligand RMSD, "Ligfit Prot"

shows the ligand's RMSD in the plot above. If the data provided are significantly higher than the protein's RMSD, the ligand has most likely disseminated away from its initial interaction site. The results showed that the complexes under investigation exhibited appropriate range across the MD trajectories and stable interactions.

4.2.3.2 RMSF Analysis

The Root Mean Square Fluctuation (RMSF) is an effective means for evaluating regional modifications throughout the protein backbone.

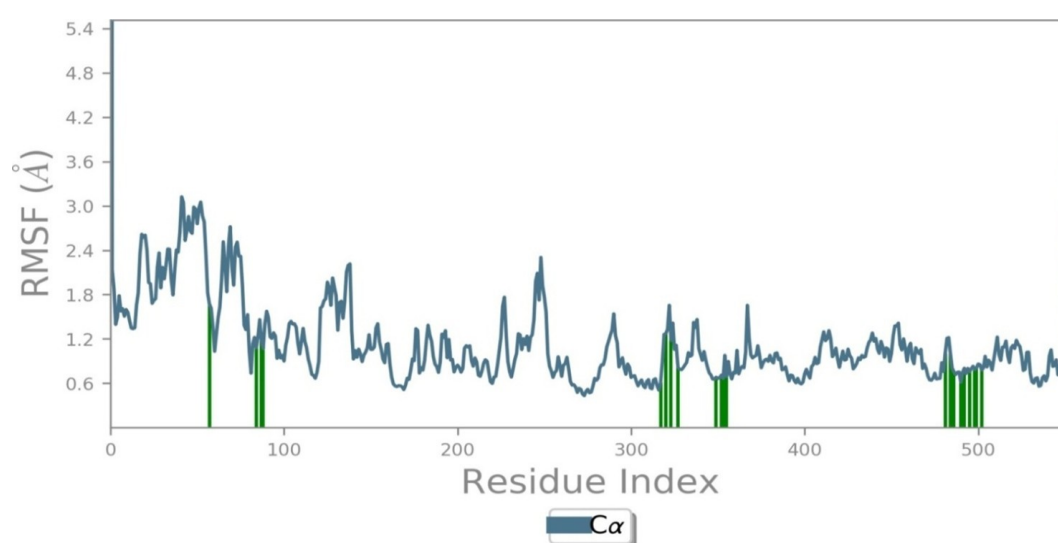


FIGURE 4.8: RMSF Analysis of compound F2 with target protein

Figure 4.8 showed that peaks on the above diagram represent the protein areas that change the most during the simulation. The N and C terminal tails of the protein usually fluctuate more than any other portion of the protein. Alpha helices and beta strands are examples of secondary structural elements that typically tend to be more stiff than the disorganized component of the protein, although they vary shorter than loop portions. Root mean square fluctuation analysis (RMSF) is used to examine the protein's movable area or structural regions that alter proportionately to the protein's overall structure. It determines the mean velocity of atoms at a specific temperature and pressure strong system, a substantial RMSF score indicates resilience. Whereas greater system flexibility is demonstrated by

a big one throughout the MD simulation. The findings indicate that RMSFs exhibited low volatility and high stability.

Ligand Contacts: Protein residues that make contact with the ligand are shown by green bars in the vertical direction.

The Ligand Root Mean Square Fluctuation (L-RMSF) can be used to characterize changes in the ligand atoms' positions. Ligand RMSF shows the variations of the ligand by atom and correlates to the two-dimensional configuration in the top panel. It could offer more about the entropic role of ligand fragments in their interactions with the protein and the binding event from the ligand RMSF. The 'Fit Ligand onto Protein' alignment in the lower panel shows the ligand variations with respect to the protein. Prior to measuring the ligand RMSF on the ligand heavy atoms, the protein ligand the integrated system is initially synchronized where the protein supported structure as shown in figure 4.9.

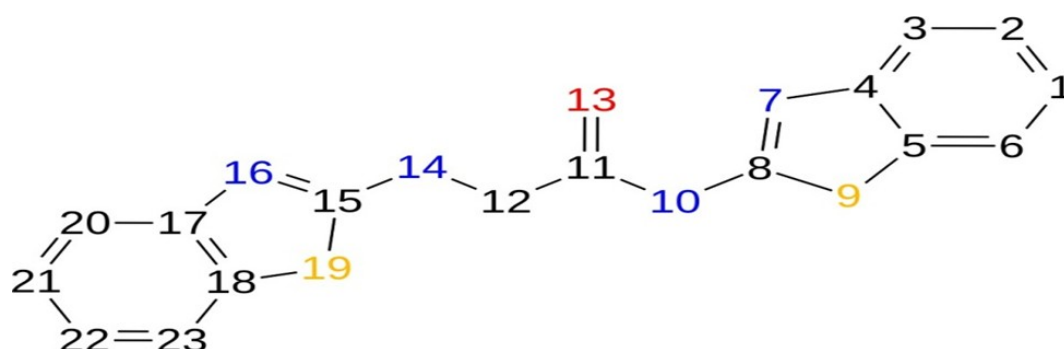


FIGURE 4.9: Protein–ligand contact of Compound F2

4.2.3.3 Protein-Ligand Contacts

Protein–ligand interactions were monitored throughout the molecular dynamics simulation and subsequently classified based on interaction type, as demonstrated in the corresponding figure. These interactions—commonly known as "contacts"—were grouped into four primary categories: hydrogen bonds, hydrophobic interactions, ionic interactions, and water bridges. Each category includes specific subtypes that can be further analyzed using the 'Simulation Interactions Schematic' module.

The resulting bar graphs represents standardized interaction frequencies over the simulation timeline; for instance, a value of 0.7 indicates that Tyr385 maintained a defined proximity to the ligand for 70% of the simulation duration. Notably, values exceeding 1.0 may occur when a single protein residue establishes multiple contacts of the same interaction type with the ligand at different time points.

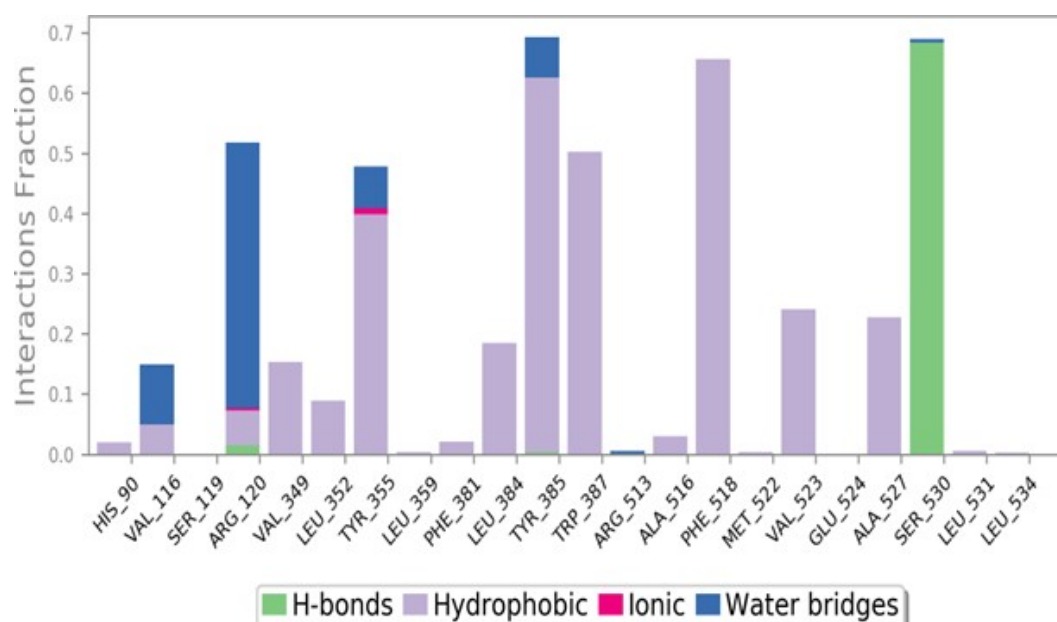


FIGURE 4.10: Interaction Fraction for the Compound F2

For ligand binding, hydrogen bonds are crucial. When creating new medications, hydrogen-bonding characteristics should be considered since they significantly affect drug selectivity, metabolization, and adsorption. There are four kinds of hydrogen bonding that form between a ligand and a protein: backbone donor, backbone acceptor, side-chain acceptor, and side-chain donor. The current geometric requirements for protein-ligand H-bonds are as follows: the donor and acceptor atoms must be 2.5 Å apart ($DH\bullet\bullet\bullet A$), the donor and hydrogen-acceptor atoms must be 120° apart ($D-H\bullet\bullet\bullet A$), and the hydrogen-acceptor-bonded atoms must be 90° apart ($H\bullet\bullet\bullet A-X$).

It comes into three subtypes: non-specific interactions, -cation. These interactions generally involve an aromatic or aliphatic moiety of the ligand interacting with amino acid hydrophobic residues. However, in this analysis, the classification has been broadened to also encompass cation- π interactions. The current geometric

criteria for hydrophobic interactions are as follows: -cation—Characteristic and aromatic groups near 4.5 Å; Other: A generic hydrophobic side chain beyond 3.6 Å of a ligand's aromatic or aliphatic carbons; two aromatic groups stacked adjacent to one another or face-to-edge. Ionic interaction or polar interactions, take place between two contrary charged atoms that are near 3.7 Å of one another and do not entail a hydrogen bond. Additionally, upon observing the protein-protein interaction, metals, and ligands, it shows a metal ion as a characteristic that is positioned between 3.4 Å of the ligand and protein's powerful atoms (apart from carbon). There are two categories of ionic interactions: those mediated by side chains or the backbone of proteins. Interactions between hydrogen-bonded proteins and ligands that are made possible by a water molecule are known as water bridges. Compared to conventional H-bonding definition, the hydrogen bonding geometry is somewhat loosened.

The geometric criteria for defining hydrogen bonds between protein and water or water and ligand atoms include a donor-acceptor distance (D-H...A) of 2.8 Å. Additionally, the sequence of molecular contacts and interactions—such as water bridges, ionic interactions, hydrophobic contacts, and hydrogen bonds—were systematically characterized as detailed on the preceding page. Figure 4.10 showed that the top panel shows the total number of unique contacts the protein has with the ligand during the journey. The lower panel shows remnants that have interactions to the ligand in every tracking frame. A darker orange hue on the plot's right-hand scale denotes that some residues make several different interactions with the ligand.

4.2.3.4 *Ligand Protein Contacts*

Due to fact some residues may possess several contacts with the ligand atom of the same kind, interactions with >100% are feasible. For example, figure 4.11 demonstrated that the side chain of an Arginine (ARG) residue contains four hydrogen bond donor sites, all of which are capable of forming hydrogen bonds with a single hydrogen bond acceptor.

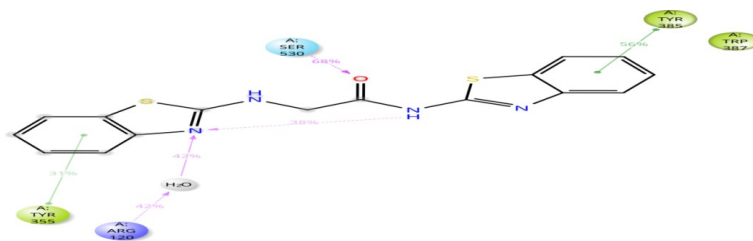


FIGURE 4.11: Ligand protein Contact of Compound F2

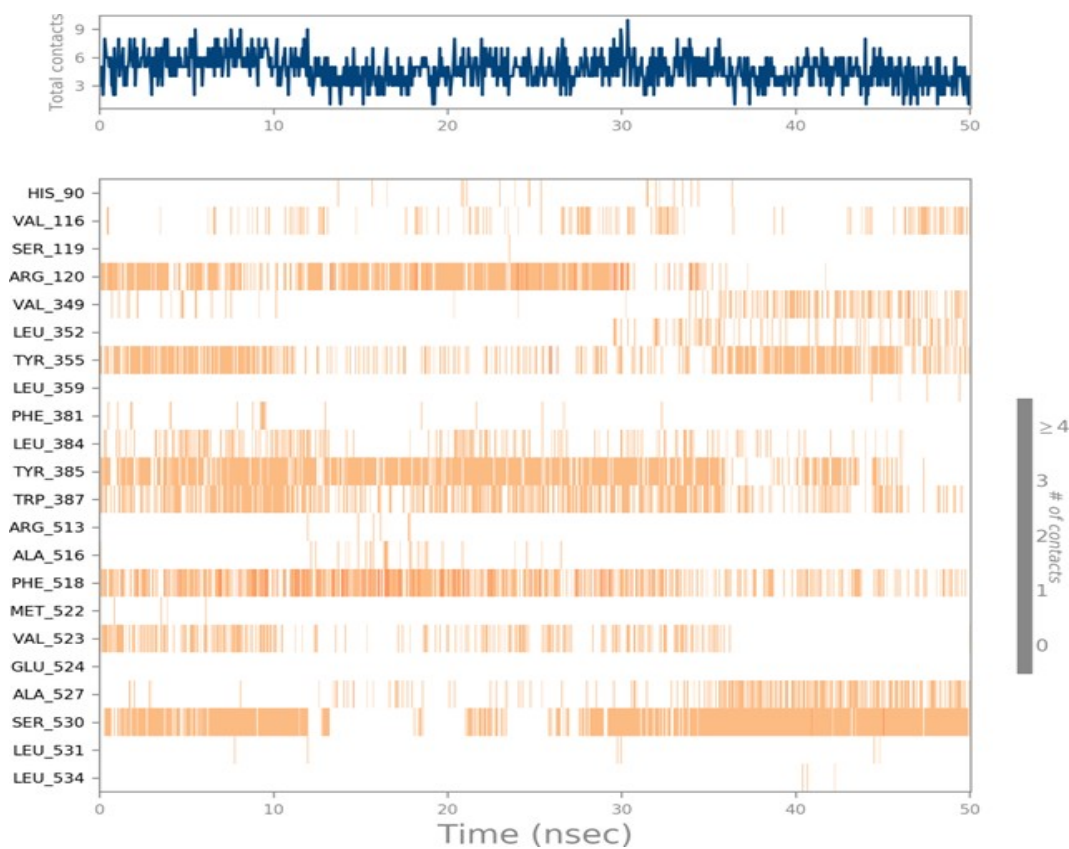


FIGURE 4.12: The precise interactions between the protein residues and the ligand atoms

Figure 4.12 showed that over 30.0% of the simulation time, encounters that occur in the selected pathway (0.00 through 50.05 nsec) are shown.

4.2.3.5 Ligand Torsion Profile

The ligand torsion analysis encapsulates the structural of each movable bond throughout the simulation pathway spanning 0.00 to 50.05 ns. Figure 4.13 demonstrated that the upper panel displays a two-dimensional schematic of the ligand

that has rotatable bonds that are colored. Bar graphs and related dial (radial) plots in matching hues are supplied for every rotatable bond. The dial plots illustrate the torsion angle conformations throughout time, starting from the center of the radial plot and progressing exterior to represent the temporal evolution. Bar plots depict the degree of plausibility distribution the effect of torsional angles, offering a summary of the dial chart data. When data on torsional probable are available, the plot additionally displays potential energy profile (sum of associated torsions) for each rotatable bond, with readings on the far left Y-axis, displayed in kcal/mol.

Correlating the torsional potential with the histogram data enables assessment of the conformational stress that the ligand endures while preserving its protein-bound conformation.

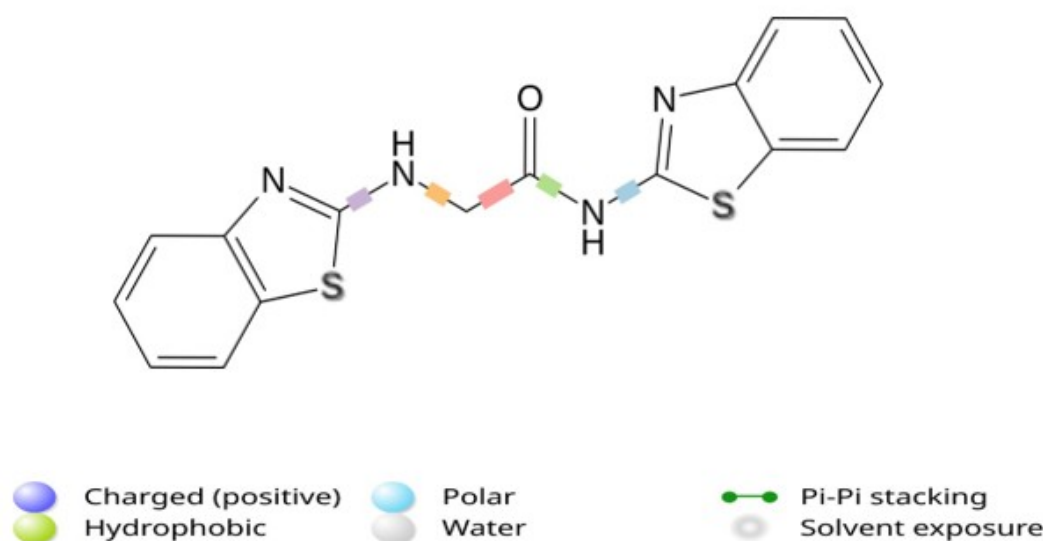


FIGURE 4.13: Ligand Torsion Profile of Compound F2

4.2.4 Cheminformatics Properties of Synthesized Compounds

The synthesized compounds F1 and F2 exhibit favorable drug-like traits while following Lipinski's Rule of Five (Ro5) with zero contravention, as evidenced by their

molecular weight (F1: 228.70, F2: 344.46; both <500), lipophilicity (F1: miLogP 1.72, F2: 3.09; both <5), hydrogen bond donors (F1: 2, F2: 4; ≤ 5), and acceptors (F1: 3, F2: 5; ≤ 10). F1 demonstrates better solubility and absorption potential due to its lower miLogP and TPSA (41.12 Å² vs. F2's 65.18 Å²), while F2, with a higher rotatable bond count (4 vs. 2), may exhibit greater flexibility but remains within Veber's rule thresholds (TPSA <140 Å², rotatable bonds ≤ 10). Both compounds are promising candidates for further optimization in drug development (Table 4.5).

TABLE 4.5: Cheminformatics properties of Synthesized Compounds

S.N	Mol-Chemo informatics Properties	F1	F2
01	MiLogP	1.72	3.09
02	TPSA	41.12	65.18
03	Natoms	14	23
04	MW	228.70	344.46
05	Non	3	5
06	Nohnh	2	4
07	Nviolations	0	0
08	Nrotb	2	4
09	Volume	182.28	289.08

4.3 *In Vitro* Studies

4.3.1 *Anti-Oxidant Assay*

Antioxidant potential of newly synthesized compounds F1 and F2 were assessed using ascorbic acid and the DPPH (1,1-diphenyl-2-picrylhydrazyl) free radical assay. (AA) as the positive control. The purple DPPH solution ($\lambda_{\text{max}} = 517 \text{ nm}$)

decolorizes to yellow when neutralized by antioxidants through hydrogen atom or electron donation. As shown in figure 4.14, compound F2 exhibited dose-dependent scavenging activity, with near-complete inhibition ($90.50 \pm 0.50\%$) at $1000 \mu\text{g/mL}$, comparable to ascorbic acid. The IC_{50} value of F2 ($302.3 \mu\text{g/mL}$) approached that of AA ($226.9 \mu\text{g/mL}$), confirming its potent free radical scavenging capacity. These results highlight F2 as a promising antioxidant agent.

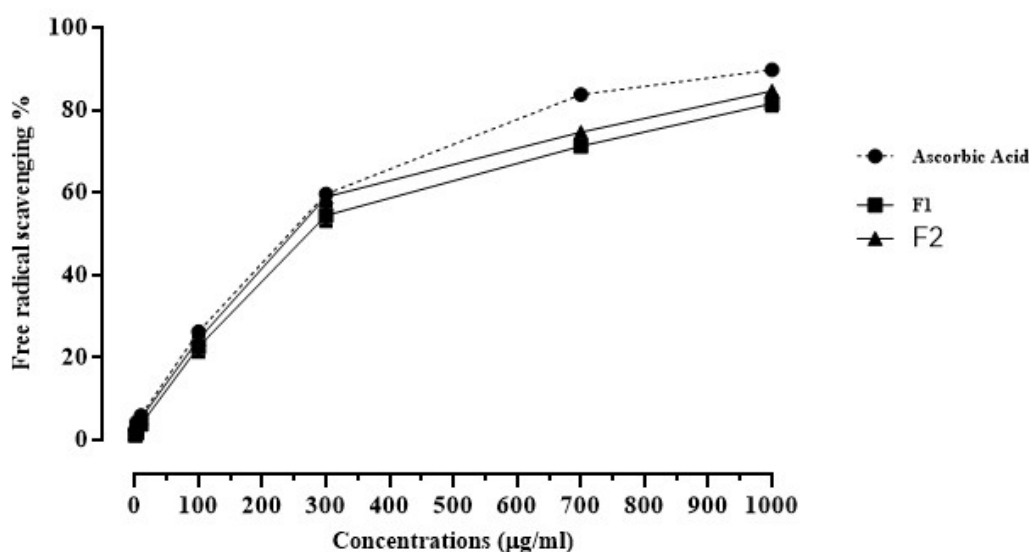


FIGURE 4.14: Percentage free radical scavenging activity by DPPH for synthesized Compound F1 and F2 (Mean \pm SEM).

Antioxidant benzothiazole derivatives, especially those incorporating Phenolic groups, show dual functionality in combating oxidative stress while maintaining other therapeutic properties. This multifunctionality is particularly valuable in neurodegenerative disease treatment, where oxidative damage contributes a crucial pathological function.

The antiviral prospect of benzothiazole substances has been convincingly demonstrated against influenza strains, with certain derivatives outperforming standard treatments like oseltamivir in experimental models [86]. The antioxidant capacity of 2-amino benzothiazole Schiff bases, particularly in neural protection contexts, further expands the therapeutic potential of this chemical class. While activity levels vary among derivatives, the consistent demonstration of radical scavenging

capabilities across multiple assay systems confirms the intrinsic redox-modulating properties of benzothiazole architectures [52].

This comprehensive pharmacological profile, combined with opportunities for structural optimization through modern synthetic approaches, establishes benzothiazole derivatives as a cornerstone in the development of next-generation therapeutics across multiple disease domains [87].

A series of indole-hydrazones, benzofuran-hydrazones, benzimidazole-hydrazones, arylbenzimidazoles, and benzothiazole derivatives were created and assessed for their antioxidant and antitumor properties [88]. These compounds exhibited potent antioxidant effects along with promising photoprotective and anticancer activities. Notably, compound 25 demonstrated significant antifungal activity against dermatophytes (IC = 2 $\mu\text{g}/\text{mL}$) and strong antioxidant performance in DPPH and FRAP assays. Additionally, it showed potent cytotoxicity against human melanoma cells, with an IC₅₀ of 9.7 μM [31].

4.4 *In Vivo* Studies

4.4.1 Induction of Carragenan Triggered Inflammatory Pain and Thermal Hyperalgesia Study

Male adult mice (n=4/group) were pretreated intraperitoneally with vehicle, negative control, diclofenac (3 mg/kg, positive control), and F1 and F2 (10 mg/kg) 30 minutes prior to carrageenan injection. Thermal hyperalgesia was assessed via hot plate test ($54\pm 1^\circ\text{C}$) at baseline and 1-3 hours post-inflammation.

F1 and F2 demonstrated time-dependent analgesic effects, significantly increasing withdrawal latency at all time points ($p < 0.05-0.01$ vs control) and outperforming Diclofenac at 3 hours as shown in figure 4.15. Vehicle-treated mice showed minimal analgesia throughout. Data (mean \pm SEM) were examined using Turkey's post-hoc test and one-way ANOVA.

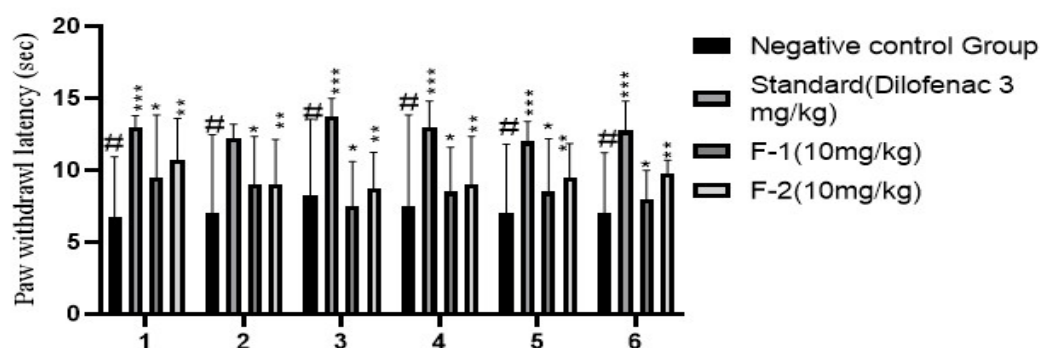


FIGURE 4.15: Carrageenan-Induced Thermal Hyperalgesia for negative, positive controls, and treatment groups (F1 and F2) $n=4$, Data (mean \pm SEM) were analyzed by one-way ANOVA with Tukey's post-hoc test, ($p<0.05$ - 0.01 vs control)

The analgesic efficacy of F2 was evaluated using a hot plate test ($54\pm 1^\circ\text{C}$) at baseline and 1–3 hours post-inflammation induction. The compound exhibited a time-dependent reduction in thermal hyperalgesia, significantly prolonging paw withdrawal latency at all measured intervals ($p<0.05$ – 0.01 compared to control) and surpassing the effect of Diclofenac at the 3-hour mark [89].

The analgesic potential of BT derivatives had been systematically explored, concerning links between structure and activity revealing that specific functional group modifications, particularly ester, fluoro, and nitrile substitutions, significantly enhance pain-relieving properties. These findings underscore the importance of molecular tailoring in optimizing therapeutic outcomes. In metabolic disorders, benzothiazole-based compounds demonstrate remarkable antidiabetic effects through multiple pathways, including α -amylase inhibition, PPAR agonism, and AMPK-mediated glucose uptake enhancement, with some derivatives showing superior efficacy to standard treatments [90].

4.4.2 Anti-Inflammatory Action of F2 Against Carrageenan Induced Paw Inflammation

Adult male mice ($n=4$ /group) pretreated with vehicle (3% DMSO/1.5% Tween-80), Diclofenac (3 mg/kg), compounds F1 and F2 (10 mg/kg) received intraplantar

carrageenan. Paw thickness increased significantly in controls (2.07 ± 0.07 to 4.32 ± 0.2 mm at 3h). F2 demonstrated potent anti-inflammatory activity, reducing edema to 3.21 ± 0.2 mm ($p < 0.001$ vs control), comparable to Diclofenac (3.36 ± 0.06 mm) in figure 4.16. Vehicle-treated mice showed no significant anti-inflammatory effects.

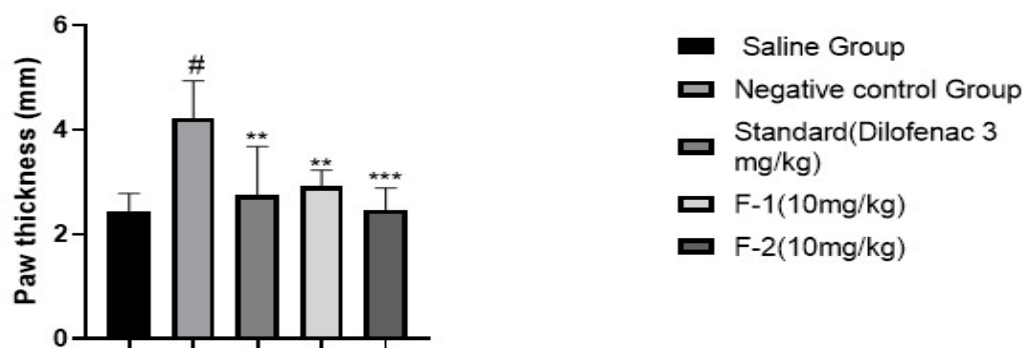


FIGURE 4.16: Anti-Inflammatory activity by Carrageenan-Induced Paw Inflammation for negative, positive controls, and treatment groups (F1 and F2) $n=4$, Data (mean \pm SEM) were examined using Tukey's post-hoc test and one-way ANOVA ($p < 0.01-0.001$ vs control)

Inflammatory edema was assessed through paw thickness measurements, which increased markedly in control animals (from 2.07 ± 0.07 mm to 4.32 ± 0.2 mm at 3 hours). F2 displayed strong anti-inflammatory activity, significantly attenuating swelling to 3.21 ± 0.2 mm ($p < 0.001$ vs control), an effect comparable to that of Diclofenac (3.36 ± 0.06 mm). These findings suggest that F2 possesses significant anti-inflammatory activity.

Several novel benzothiazole derivatives, including 2-(4-butyl-3,5-dimethylpyrazol-1-yl) and 4-butyl-1-(6-substituted-2-benzothiazolyl) benzothiazoles with substitutions at the 6-position, were synthesized for anti-inflammatory applications. Among these, compound 18 demonstrated strong anti-inflammatory activity [91]. Additionally, a newly developed 2-aminobenzothiazole derivative, compound 19, was evaluated due of its ability to reduce inflammation. The investigation found that introducing electron-withdrawing groups ($-\text{Cl}$, $-\text{NO}_2$, or $-\text{OCH}_3$) at the 4- or 5-positions of the 2-aminobenzothiazole scaffold significantly enhanced its anti-inflammatory effects [92]. Anti-inflammatory properties, with efficacy rivalling established reference drugs [54]

4.4.3 *In Vivo* Acute Toxicity Assessment

The study involved twelve mice separated into three groups, each with four members. As the control, Group A was given 1 mL/10 g of body weight of 0.9% saline.

TABLE 4.6: Effects of Oral Administration of Compounds F1 and F2 on Body Weight, Consumption, and Toxicity Parameters (Mean \pm SEM)

Parameter	Time (Days)	Group A (Con- trol)	Group B (F1- Treated)	Group C (F2- Treated)
Body Weight (g)	01	32 \pm 0.86	30 \pm 0.96	31 \pm 0.94
	07	33 \pm 0.93	31 \pm 0.18	32 \pm 1.19
	14	34 \pm 4.13	32 \pm 0.42	33 \pm 0.42
Water Intake (mL/day)	01	4.8 \pm 0.60	4.1 \pm 0.44	4.5 \pm 0.44
	07	5 \pm 1.96	4.8 \pm 2.15	5.8 \pm 2.15
	14	7 \pm 2.11	5.5 \pm 2.25	7 \pm 2.25
Food Intake (g/day)	01	3 \pm 0.55	3 \pm 1.43	3 \pm 1.43
	07	4 \pm 0.54	3.5 \pm 0.81	5 \pm 0.81
	14	5 \pm 0.49	4.5 \pm 0.40	6 \pm 0.40
Toxicity	14	None	None	None

Orally, Group B was administered the synthesized compound F1 at a dose of 10 mg/kg body weight, while Group C was administered the synthesized compound F2 at a dose of 10 mg/kg body weight. All groups had availability to water and a balanced food. Over 14 days, their behavior was monitored. After the mice were put to death throughout the experiment, via cervical dislocation, and The stomach, liver, kidney, and heart were removed, cleaned, sectioned, and hematoxylin-eosin-stained for histopathological evaluation. Fig 4.17 summarizes the effects of synthesized oral F1 and F2 administration on behavior, food and water consumption, body weight, and signs of toxicity in the control group (Group A) and the

treated groups (Group B and Group C) mice. All groups exhibited normal behavior, responding appropriately to sound, light, and stimuli. No adverse effects such as salivation, vomiting, lacrimation, nasal discharge, dry mouth, edema, or abnormal feces (mucus/blood) were observed. Additionally, eating patterns remained consistent between groups, indicating no significant toxicity.

Histopathological analysis of vital organs (kidney, spleen, stomach, lungs, liver, and heart) revealed no abnormalities in the treated group. The heart exhibited normal pericardium, myocardium, and endocardium; the stomach lining showed no ulcerative lesions; and the lungs displayed no vascular thickening around the bronchi. Kidneys and spleen maintained normal size and structure, while liver lobules in the treated group had clear, well-defined boundaries, identical to controls as illustrated in figure 4.17. Collectively, these findings confirm that compounds F1 and F2 induced no adverse histopathological effects, supporting their non-toxic nature.

A comprehensive histopathological examination was conducted on all major organ systems, including the heart, liver, stomach, lungs, spleen, and kidneys, to evaluate potential toxicological effects following treatment with F1 and F2 compounds. Microscopic analysis revealed complete preservation of normal histological architecture across all examined tissues, with no evidence of pathological alterations in any treatment group when compared to control specimens. Cardiac tissue maintained its characteristic organization, with intact pericardial, myocardial, and endocardial layers showing normal cellular morphology and no signs of inflammatory infiltration, fibrosis, or degenerative changes. Hepatic architecture remained undisturbed, with clearly demarcated lobules, patent central veins, and normal portal triads, while hepatocytes exhibited their typical polyhedral shape with well-preserved cytoplasmic and nuclear features.

The gastrointestinal assessment showed complete integrity of gastric mucosa with no indications of erosion, ulceration, or hemorrhagic lesions, and all epithelial layers maintained their standard stratification. Pulmonary evaluation demonstrated normal alveolar septation without thickening or inflammatory cell accumulation,

and bronchial structures appeared with their characteristic epithelial lining and patent lumens. Renal parenchyma displayed preserved cortical and medullary organization, with glomeruli maintaining their tufted capillary networks and tubules showing intact brush borders and luminal patency. Splenic tissue exhibited normal distribution of red and white pulp components without evidence of congestion, extramedullary hematopoiesis, or lymphoid depletion.

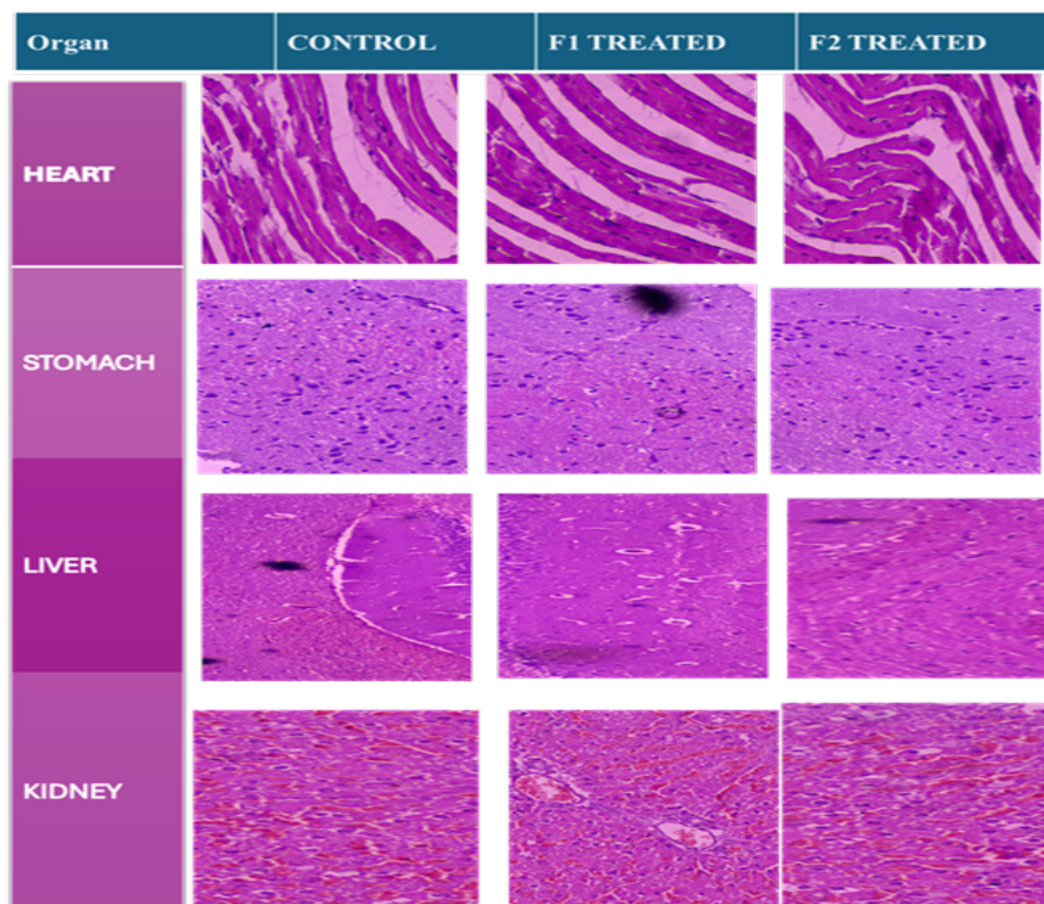


FIGURE 4.17: Histopathology of Vital Organs (heart, stomach, liver, and kidney) of treated animals, compared to control in Acute Toxicity study for synthesized compounds F1 and F2

These histomorphological findings were quantitatively and qualitatively indistinguishable from control specimens, as clearly illustrated in Figure 4.16 confirming the absence of any treatment-related pathological changes. The comprehensive preservation of micro anatomical features across all vital organ systems provides definitive evidence that both F1 and F2 compounds induce no detectable adverse effects at the cellular or tissue level. This thorough histopathological correlation

strongly supports the safety profile indicated by previous gross toxicity assessments, reinforcing the conclusion that these compounds exhibit no organ-specific toxicity under the experimental conditions employed. The absence of any degenerative, inflammatory, or proliferative abnormalities in these critical organ systems substantiates the potential therapeutic applicability of these compounds without anticipated histotoxic consequences.

The study evaluated the safety of compounds F1 and F2 (10 mg/kg, orally) in mice over 14 days, compared to a saline control. F2-treated mice showed no behavioral abnormalities, toxicity symptoms (e.g., vomiting, edema), or changes in food/water intake, similar to controls [93]. Histopathological analysis revealed no organ damage—heart, liver, kidneys, stomach structure indistinguishable from controls. These results confirm F2's non-toxic profile, supporting its potential for further pharmacological development [88].

Benzothiazole (BTA) and derivations of it signify for a highly worthwhile class of heterocyclic substances that are extensively distributed in natural products and pharmaceutical agents. These compounds exhibit remarkable structural diversity, enabling their incorporation into numerous drug development programs [27]. The benzothiazole scaffold has demonstrated an impressive array of pharmacological activities, making it a privileged structure in medicinal chemistry. Recent decades have encountered accelerated advancement in technical innovation of BTA-containing therapeutics, with these compounds showing particular promise in addressing diverse pathological conditions [94]. The pharmacological profile of BTA derivatives encompasses anticancer, antimicrobial, anti-inflammatory, analgesic, and antioxidant properties, along with notable activity against tuberculosis, diabetes, malaria, and convulsive disorders. This broad spectrum of biological activities has positioned BTA derivatives as valuable templates for drug discovery [95]. Current research efforts are increasingly focused on optimizing BTA-based compounds to enhance their therapeutic efficacy while minimizing potential toxicity. The continuous exploration of novel BTA derivatives reflects the pharmaceutical community's commitment to developing more potent, selective, and safer therapeutic agents [96]. These advancements underscore the growing importance

of benzothiazole derivatives in modern drug development and their potential to address various unmet medical needs. The structural versatility of the benzothiazole nucleus continues to inspire innovative approaches in the design of diagnostic and therapeutic agents, promising significant contributions to future pharmacotherapy [87].

Past few decades had perceived notable growth in research and development of benzothiazole (BF₂)-based pharmaceutical compounds, establishing this field as a dynamic and rapidly evolving area of medicinal chemistry. A wide array of benzothiazole-containing compounds have demonstrated remarkable therapeutic potential against diverse diseases [97]. This examination focuses on contemporary advances in synthesizing benzothiazole analogues, particularly emphasizing environmentally sustainable green chemistry approaches. Through comprehensive analysis of scientific literature from national and international journals, books, and digital resources, it becomes evident that the structural versatility of the benzothiazole core enables diverse pharmacological applications [98].

The therapeutic scope of benzothiazole derivatives spans multiple medical domains, including antimicrobial treatments, hepatitis C virus inhibition, management of alzheimer's disease, pain and inflammation relief, oxidative stress reduction, seizure control, diabetes treatment, allergy management, malaria therapy, and mood disorder treatment.

Chapter 5

Conclusion and Future Prospects

The present study highlights the successful development of two novel benzothiazole derivatives, F1 and F2 with F2 emerging as a particularly promising multifunctional therapeutic agent. Its strong COX-2 binding affinity (-7.5 kcal/mol), potent anti-inflammatory and analgesic effects (surpassing diclofenac in prolonged anti-inflammatory activity), and significant antioxidant capacity ($IC_{50} = 302.3$ g/mL) position it as a viable candidate for treating oxidative stress-associated inflammatory disorders. The protein-ligand complex's molecular dynamics simulation (`desmond_md_job_F2.5KIR`) revealed stable binding interactions, with the ligand exhibiting low RMSD fluctuations ($\sim 1-2$ Å) and key residues (e.g., SER_530, TYR_355) maintaining consistent contacts. The system equilibrated effectively, demonstrating structural integrity and potential for further drug development. Importantly, F2 demonstrated an excellent safety profile in acute toxicity studies, with no adverse effects on vital organs or physiological parameters. These findings reinforce the benzothiazole scaffold's versatility in drug design and its potential to yield safer, more effective alternatives to conventional therapeutics.

Future research should focus on optimizing F2's pharmacokinetic properties through structural modifications to enhance bioavailability and target selectivity. In-depth mechanistic studies are needed to elucidate its anti-inflammatory pathways, particularly its interaction with COX-2 and redox-modulating mechanisms. Chronic toxicity evaluations and *in vivo* efficacy studies in disease models

(e.g., rheumatoid arthritis or neurodegenerative disorders) would further validate its clinical potential. Additionally, formulation development for improved delivery and combination studies with existing drugs could broaden its therapeutic applications. The robust activity and low toxicity of F2 underscore its promise as a lead compound for developing next-generation anti-inflammatory-antioxidant hybrid drugs.

Bibliography

- [1] P. Martins *et al.*, “Heterocyclic anticancer compounds: Recent advances and the paradigm shift towards the use of nanomedicine’s tool box,” *Molecules*, vol. 20, no. 9, pp. 16852–16891, 2015.
- [2] P. Arora, V. Arora, H. Lamba, and D. Wadhwa, “Importance of heterocyclic chemistry: A review,” *International Journal of Pharmaceutical Sciences and Research*, vol. 3, no. 9, p. 2947, 2012.
- [3] D. Kumar and S. Kumar Jain, “A comprehensive review of n-heterocycles as cytotoxic agents,” *Current Medicinal Chemistry*, vol. 23, no. 38, pp. 4338–4394, 2016.
- [4] G. Verma, M. Shaquiquzzaman, and M. M. Alam, “Heterocyclic drug design and development,” in *Promising Drug Molecules of Natural Origin*, pp. 271–333, Apple Academic Press, 2020.
- [5] N. D. Mahajan and N. Jain, “Heterocyclic compounds and their applications in the field of biology: A detailed study,” *NVEO-Natural Volatiles & Essential Oils Journal*, pp. 13223–13229, 2021.
- [6] E. Kabir and M. Uzzaman, “A review on biological and medicinal impact of heterocyclic compounds,” *Results in Chemistry*, vol. 4, p. 100606, 2022.
- [7] M. Ibragimova, “Analysis of heterocyclic compounds,” *Science and Innovation*, vol. 1, no. 4, pp. 266–268, 2022.

- [8] M. Bedair, "The effect of structure parameters on the corrosion inhibition effect of some heterocyclic nitrogen organic compounds," *Journal of Molecular Liquids*, vol. 219, pp. 128–141, 2016.
- [9] O. Ebenezer, M. A. Jordaan, G. Carena, T. Bono, M. Shapi, and J. A. Tuszynski, "An overview of the biological evaluation of selected nitrogen-containing heterocycle medicinal chemistry compounds," *International Journal of Molecular Sciences*, vol. 23, no. 15, p. 8117, 2022.
- [10] T. Abd Rehan, "Review on different five-membered heterocyclic aromatic compounds and their pharmaceutical applications," *Global Scientific Journal (GSJ)*, vol. 12, no. 6, 2024.
- [11] S. Tiwari and S. Talreja, "A study on aromatic heterocyclic organic compounds," *Journal of Pharmaceutical Research International*, vol. 34, no. 41B, pp. 36–40, 2022.
- [12] A. T. Balaban, D. C. Oniciu, and A. R. Katritzky, "Aromaticity as a cornerstone of heterocyclic chemistry," *Chemical Reviews*, vol. 104, no. 5, pp. 2777–2812, 2004.
- [13] J. Alvarez-Builla and J. Barluenga, "Heterocyclic compounds: An introduction," in *Modern Heterocyclic Chemistry*, pp. 1–9, 2011.
- [14] S. Jaiswal, "Five and six membered heterocyclic compound with antimicrobial activity," *Journal of Modern Trends in Science and Technology*, vol. 5, pp. 36–39, 2019.
- [15] N. Kerru, L. Gummidi, S. Maddila, K. K. Gangu, and S. B. Jonnalagadda, "A review on recent advances in nitrogen-containing molecules and their biological applications," *Molecules*, vol. 25, no. 8, p. 1909, 2020.
- [16] N. Korol, D. Molnar-Babilya, M. Slivka, and M. Onysko, "A brief review on heterocyclic compounds with promising antifungal activity against candida species," 2022. No journal information available.

- [17] S. K. Rastogi, V. C. Ciliberto, M. Z. Trevino, B. A. Campbell, and W. J. Brittain, "Green approach toward triazole forming reactions for developing anticancer drugs," *Current Organic Synthesis*, vol. 21, no. 4, pp. 380–420, 2024.
- [18] P. K. Singh and O. Silakari, "Multitargeting heterocycles: Improved and rational chemical probes for multifactorial diseases," in *Key Heterocycle Cores for Designing Multitargeting Molecules*, pp. 1–29, Elsevier, 2018.
- [19] M. Mantzanidou, E. Pontiki, and D. Hadjipavlou-Litina, "Pyrazoles and pyrazolines as anti-inflammatory agents," *Molecules*, vol. 26, no. 11, p. 3439, 2021.
- [20] I. Khan, S. Zaib, and A. Ibrar, "New frontiers in the transition-metal-free synthesis of heterocycles from alkynoates: An overview and current status," *Organic Chemistry Frontiers*, vol. 7, no. 22, pp. 3734–3791, 2020.
- [21] C. Rizzo, A. Pace, I. Pibiri, S. Buscemi, and A. Palumbo Piccionello, "From conventional to sustainable catalytic approaches for heterocycles synthesis," *ChemSusChem*, vol. 17, no. 8, p. e202301604, 2024.
- [22] M. García-Valverde and T. Torroba, "Sulfur-nitrogen heterocycles," *Molecules*, vol. 10, no. 2, pp. 318–320, 2005.
- [23] S. M. Alsafy and N. A. Alrazzak, "Synthesis, characterization, and biological activity study of new heterocyclic compounds," *Engineering Proceedings*, vol. 59, no. 1, p. 178, 2023.
- [24] M. Asif and M. Imran, "A chapter on synthesis of various heterocyclic compounds by environmentally friendly green chemistry technologies," in *Handbook of Greener Synthesis of Nanomaterials and Compounds*, pp. 69–108, 2021.
- [25] C. S. W. Law and K. Y. Yeong, "Current trends of benzothiazoles in drug discovery: A patent review (2015–2020)," *Expert Opinion on Therapeutic Patents*, vol. 32, no. 3, pp. 299–315, 2022.

- [26] M. Gjorgjieva, T. Tomašič, D. Kikelj, and L. P. Mašič, “Benzothiazole-based compounds in antibacterial drug discovery,” *Current Medicinal Chemistry*, vol. 25, no. 38, pp. 5218–5236, 2018.
- [27] A. Irfan *et al.*, “Benzothiazole derivatives as anticancer agents,” *Journal of Enzyme Inhibition and Medicinal Chemistry*, vol. 35, no. 1, pp. 265–279, 2020.
- [28] M. Bhat and S. L. Belagali, “Structural activity relationship and importance of benzothiazole derivatives in medicinal chemistry: A comprehensive review,” *Mini-Reviews in Organic Chemistry*, vol. 17, no. 3, pp. 323–350, 2020.
- [29] S. Sulthana and P. Pandian, “A review on indole and benzothiazole derivatives its importance,” *Journal of Drug Delivery and Therapeutics*, vol. 9, pp. 505–509, 2019.
- [30] P. Prajapat, “Importance of benzothiazole motif in modern drug discovery: Introduction,” *Organic Chemistry*, vol. 8, no. 2, pp. 1795–1801, 2012.
- [31] K. P. Yadav, M. A. Rahman, S. Nishad, S. K. Maurya, M. Anas, and M. Mujahid, “Synthesis and biological activities of benzothiazole derivatives: A review,” *Intelligent Pharmacy*, vol. 1, no. 3, pp. 122–132, 2023.
- [32] L. V. Zhilitskaya, B. A. Shainyan, and N. O. Yarosh, “Modern approaches to the synthesis and transformations of practically valuable benzothiazole derivatives,” *Molecules*, vol. 26, no. 8, p. 2190, 2021.
- [33] N. Saha, A. Kumar, B. B. Debnath, A. Sarkar, and A. K. Chakraborti, “Recent advances in the development of greener methodologies for the synthesis of benzothiazoles,” *Current Topics in Medicinal Chemistry*, vol. 25, no. 5, pp. 581–644, 2025.
- [34] N. Saha, “1.2.3 sustainable reaction approaches/strategies,” in *Aqueous-Mediated Synthesis: Bioactive Heterocycles*, vol. 2, p. 12, 2024.

- [35] M. Ozdincer, A. Dalmaz, S. Durmus, G. Dulger, and I. Kiliccioglu, "Biological evaluation of benzothiazoles obtained by microwave-green synthesis," *Anais da Academia Brasileira de Ciências*, vol. 96, no. suppl 1, p. e20230423, 2024.
- [36] V. Sagar and A. Sarkar, "Biological activity of substituted benzothiazoles," *Asian Journal of Research in Chemistry*, vol. 17, no. 5, pp. 289–295, 2024.
- [37] Z. Khalifa, R. Upadhyay, and A. B. Patel, "Benzothiazole derivatives as effective -glucosidase inhibitors: An insight study of structure-activity relationships and molecular targets," *Medicinal Chemistry Research*, vol. 33, no. 12, pp. 2347–2371, 2024.
- [38] N. Saha, S. Biswas, S. Naskar, A. Sarkar, and A. K. Chakraborti, "Microwave-assisted solvent-free synthesis of benzazoles," in *Solvent-Free Synthesis: Bioactive Heterocycles*, vol. 4, p. 17, 2023.
- [39] K. Kant *et al.*, "Recent advancements in strategies for the synthesis of imidazoles, thiazoles, oxazoles, and benzimidazoles," *ChemistrySelect*, vol. 8, no. 47, p. e202303988, 2023.
- [40] S. S. Panda, R. Malik, and S. C. Jain, "Synthetic approaches to 2-arylbenzimidazoles: A review," *Current Organic Chemistry*, vol. 16, no. 16, pp. 1905–1919, 2012.
- [41] A. Gupta, "Antifungal activity of novel c-6 methyl substituted benzothiazole derivatives against *candida albicans*," *Journal of Cosmetology and Trichology*, vol. 4, no. 2, p. 2, 2018.
- [42] N. Bhoge, B. Magare, and P. Mohite, "Synthesis and biological evaluation of 3-(benzo[d]thiazol-2-yl)-2-(substituted aryl)thiazolidin-4-one derivatives," 2023. Journal details not provided.
- [43] A. Mondal, R. Sharma, D. Pal, and D. Srimani, "Recent progress in the synthesis of heterocycles through base metal-catalyzed acceptorless dehydrogenative and borrowing hydrogen approach," *European Journal of Organic Chemistry*, vol. 2021, no. 26, pp. 3690–3720, 2021.

- [44] S. S. Acharya, S. Patra, L. M. Barad, A. Roul, and B. B. Parida, "Recent advances in iodine-dmsO mediated c(sp³)-h functionalizations of methylazaarenes via Kornblum oxidation," *New Journal of Chemistry*, 2024.
- [45] P. Kumar, R. Bhatia, and N. K. Rangra, "Scaffolds imparting anthelmintic activity: Recent advancements and SAR studies," *Molecular Diversity*, vol. 29, no. 1, pp. 783–816, 2025.
- [46] U. Khan and S. Sur, "Exploring the DNA recognition of compounds based on benzimidazole and benzothiazole: A concise review," in *Macromolecular Symposia*, vol. 413, p. 2400111, Wiley Online Library, 2024.
- [47] Z.-B. Dong, Z. Gong, Q. Dou, B. Cheng, and T. Wang, "A decade update on the application of -oxodithioesters in heterocyclic synthesis," *Organic & Biomolecular Chemistry*, vol. 21, no. 34, pp. 6806–6829, 2023.
- [48] S. Radhika, M. B. Aleena, and G. Anilkumar, "A green aerobic Fe(III) catalyzed base-free synthesis of 2-aminobenzothiazoles in water," *Journal of Catalysis*, vol. 416, pp. 233–239, 2022.
- [49] V. Dhayalan *et al.*, "Recent synthetic strategies for the functionalization of fused bicyclic heteroaromatics using organo-Li, -Mg and -Zn reagents," *Chemical Society Reviews*, 2024.
- [50] P. Kashyap, S. Verma, P. Gupta, R. Narang, S. Lal, and M. Devgun, "Recent insights into antibacterial potential of benzothiazole derivatives," *Medicinal Chemistry Research*, vol. 32, no. 8, pp. 1543–1573, 2023.
- [51] K. Gupta, A. K. Sirbaiya, V. Kumar, and M. A. Rahman, "Current perspective of synthesis of medicinally relevant benzothiazole based molecules: Potential for antimicrobial and anti-inflammatory activities," *Mini Reviews in Medicinal Chemistry*, vol. 22, no. 14, pp. 1895–1935, 2022.
- [52] X. Xu *et al.*, "Synthesis and biological evaluation of novel benzothiazole derivatives as potential anticancer and anti-inflammatory agents," *Frontiers in Chemistry*, vol. 12, p. 1384301, 2024.

- [53] C. Tratratt, "Benzothiazole as a promising scaffold for the development of antifungal agents," *Current Topics in Medicinal Chemistry*, vol. 23, no. 7, pp. 491–519, 2023.
- [54] P. R. Prasad, K. Bhuvanewari, and S. Kuberkar, "Synthesis and biological activity evaluation of some fused imino pyrimido benzothiazole derivatives," *International Journal of Pharmaceutical, Chemical & Biological Sciences*, vol. 4, no. 3, 2014.
- [55] R. Hussain, S. Khan, A. Sardar, L. Rasheed, M. S. Islam, and T. M. Almutairi, "Synthetic strategies, biological and computational screening of thiadiazole bearing benzothiazole derivatives as prospective anti-diabetic agents," *Journal of Molecular Structure*, vol. 1337, p. 142141, 2025.
- [56] M. J. Ramaiah *et al.*, "Synthesis, in vitro and structural aspects of benzothiazole analogs as anti-oxidants and potential neuroprotective agents," *Environmental Toxicology and Pharmacology*, vol. 79, p. 103415, 2020.
- [57] A. Drakontaeidi, I. Papanotas, and E. Pontiki, "Multitarget pharmacology of sulfur–nitrogen heterocycles: Anticancer and antioxidant perspectives," *Antioxidants*, vol. 13, no. 8, p. 898, 2024.
- [58] E. N. Djuidje *et al.*, "Benzothiazole derivatives as multifunctional antioxidant agents for skin damage: Structure–activity relationship of a scaffold bearing a five-membered ring system," *Antioxidants*, vol. 11, no. 2, p. 407, 2022.
- [59] M. Kumar, S.-M. Chung, G. Enkhtaivan, R. V. Patel, H.-S. Shin, and B. M. Mistry, "Molecular docking studies and biological evaluation of berberine–benzothiazole derivatives as an anti-influenza agent via blocking of neuraminidase," *International Journal of Molecular Sciences*, vol. 22, no. 5, p. 2368, 2021.
- [60] L. Racané *et al.*, "Synthesis, antiproliferative and antitrypanosomal activities, and dna binding of novel 6-amidino-2-arylbenzothiazoles," *Journal of Enzyme Inhibition and Medicinal Chemistry*, vol. 36, no. 1, pp. 1952–1967, 2021.

- [61] B. A. Shainyan, L. V. Zhilitskaya, and N. O. Yarosh, "Synthetic approaches to biologically active c-2-substituted benzothiazoles," *Molecules*, vol. 27, no. 8, p. 2598, 2022.
- [62] M. Cindrić *et al.*, "Experimental and computational study of the antioxidative potential of novel nitro and amino substituted benzimidazole/benzothiazole-2-carboxamides with antiproliferative activity," *Antioxidants*, vol. 8, no. 10, p. 477, 2019.
- [63] S. H. Abdullahi *et al.*, "Molecular docking studies of some benzoxazole and benzothiazole derivatives as vegfr-2 target inhibitors: In silico design, md simulation, pharmacokinetics and dft studies," *Intelligent Pharmacy*, vol. 2, no. 2, pp. 232–250, 2024.
- [64] P. Jain, M. N. Noolvi, U. A. More, and M. B. Palkar, "Molecular docking & md simulation studies to design benzothiazole-thiazole hybrids as potent p56lck inhibitors for the treatment of cancer," 2024. Journal/publisher information not provided.
- [65] V. Ivanović, M. Rančić, B. Arsić, and A. Pavlović, "Lipinski's rule of five, famous extensions and famous exceptions," *Popular Scientific Article*, vol. 3, no. 1, pp. 171–177, 2020.
- [66] A. S. Dighe and A. E. Tajamulhaq, "An overview of molecular docking," *Asian Journal of Pharmaceutical Research*, vol. 14, no. 3, 2024.
- [67] A. Mubarik *et al.*, "Computational study of benzothiazole derivatives for conformational, thermodynamic and spectroscopic features and their potential to act as antibacterials," *Crystals*, vol. 12, no. 7, p. 912, 2022.
- [68] Z. Mirjafary, M. M. Karbasi, P. Hesamzadeh, H. R. Shaker, A. Amiri, and H. Saeidian, "Novel 1,2,3-triazole-based benzothiazole derivatives: Efficient synthesis, dft, molecular docking, and admet studies," *Molecules*, vol. 27, no. 23, p. 8555, 2022.

- [69] F. Ramzan *et al.*, “Synthesis, molecular docking, and biological evaluation of a new series of benzothiazinones and their benzothiazinyl acetate derivatives as anticancer agents against mcf-7 human breast cancer cells and as anti-inflammatory agents,” *ACS Omega*, vol. 8, no. 7, pp. 6650–6662, 2023.
- [70] O. Afzal *et al.*, “Rational design, docking, simulation, synthesis, and in vitro studies of small benzothiazole molecules as selective bace1 inhibitors,” *Journal of Biomolecular Structure and Dynamics*, pp. 1–12, 2025.
- [71] M. Taha, N. H. Ismail, S. Imran, M. Selvaraj, and F. Rahim, “Synthesis of novel inhibitors of -glucuronidase based on the benzothiazole skeleton and their molecular docking studies,” *RSC Advances*, vol. 6, no. 4, pp. 3003–3012, 2016.
- [72] M. Hernández-Rodríguez, M. C. Rosales-Hernández, J. E. Mendieta-Wejbe, M. Martínez-Archundia, and J. Correa Basurto, “Current tools and methods in molecular dynamics (md) simulations for drug design,” *Current Medicinal Chemistry*, vol. 23, no. 34, pp. 3909–3924, 2016.
- [73] R. K. Mohapatra *et al.*, “Repurposing benzimidazole and benzothiazole derivatives as potential inhibitors of sars-cov-2: Dft, qsar, molecular docking, molecular dynamics simulation, and in-silico pharmacokinetic and toxicity studies,” *Journal of King Saud University - Science*, vol. 33, no. 8, p. 101637, 2021.
- [74] H. Afzaal *et al.*, “Virtual screening and drug repositioning of fda-approved drugs from the zinc database to identify the potential htert inhibitors,” *Frontiers in Pharmacology*, vol. 13, p. 1048691, 2022.
- [75] B. Bakchi *et al.*, “An overview on applications of swissadme web tool in the design and development of anticancer, antitubercular and antimicrobial agents: a medicinal chemist’s perspective,” *Journal of Molecular Structure*, vol. 1259, p. 132712, 2022.

- [76] L. Willard *et al.*, “Vadar: a web server for quantitative evaluation of protein structure quality,” *Nucleic Acids Research*, vol. 31, no. 13, pp. 3316–3319, 2003.
- [77] O. Trott and A. J. Olson, “Autodock vina: improving the speed and accuracy of docking with a new scoring function, efficient optimization, and multi-threading,” *Journal of Computational Chemistry*, vol. 31, no. 2, pp. 455–461, 2010.
- [78] R. Altaf *et al.*, “Synthesis, biological evaluation, 2d-qsar, and molecular simulation studies of dihydropyrimidinone derivatives as alkaline phosphatase inhibitors,” *ACS Omega*, vol. 7, no. 8, pp. 7139–7154, 2022.
- [79] K. Sirivibulkovit, S. Nouanthavong, and Y. Sameenoi, “Based dpph assay for antioxidant activity analysis,” *Analytical Sciences*, vol. 34, no. 7, pp. 795–800, 2018.
- [80] A. D. Modi, A. Parekh, and Y. N. Pancholi, “Evaluating pain behaviours: Widely used mechanical and thermal methods in rodents,” *Behavioural Brain Research*, vol. 446, p. 114417, 2023.
- [81] S. J. Wijeyesakere, T. Auernhammer, A. Parks, and D. Wilson, “Profiling mechanisms that drive acute oral toxicity in mammals and its prediction via machine learning,” *Toxicological Sciences*, vol. 193, no. 1, pp. 18–30, 2023.
- [82] A. El Alami, A. El Maraghi, and H. Sdassi, “Review of synthesis process of benzoxazole and benzothiazole derivatives,” *Synthetic Communications*, vol. 54, no. 10, pp. 769–801, 2024.
- [83] S. Dallakyan and A. J. Olson, “Small-molecule library screening by docking with pyrx,” in *Chemical Biology*, pp. 243–250, Springer, 2015.
- [84] I. Aayishamma *et al.*, “Benzothiazole a privileged scaffold for cutting-edges anticancer agents: Exploring drug design, structure-activity relationship, and docking studies,” *European Journal of Medicinal Chemistry*, p. 116831, 2024.

- [85] R. S. Keri, M. R. Patil, S. A. Patil, and S. Budagumpi, "A comprehensive review in current developments of benzothiazole-based molecules in medicinal chemistry," *European Journal of Medicinal Chemistry*, vol. 89, pp. 207–251, 2015.
- [86] G. Kumar and N. Singh, "Synthesis, anti-inflammatory and analgesic evaluation of thiazole/oxazole substituted benzothiazole derivatives," *Bioorganic Chemistry*, vol. 107, p. 104608, 2021.
- [87] P. C. Sharma, A. Sinhmar, A. Sharma, H. Rajak, and D. P. Pathak, "Medicinal significance of benzothiazole scaffold: an insight view," *Journal of Enzyme Inhibition and Medicinal Chemistry*, vol. 28, no. 2, pp. 240–266, 2013.
- [88] R. K. Yadav *et al.*, "Recent insights on synthetic methods and pharmacological potential in relation with structure of benzothiazoles," *Medicinal Chemistry*, vol. 19, no. 4, pp. 325–360, 2023.
- [89] A. Kumar, A. K. Shakya, and H. Siddiqui, "Synthesis and anti-inflammatory activity of some novel 2-aminobenzothiazole derivatives," *Indian Journal of Heterocyclic Chemistry*, vol. 25, pp. 243–249, 2016.
- [90] P. Venkatesh, "Synthesis, characterisation and anti-inflammatory activity of some 2-amino benzothiazole derivatives," *International Journal of ChemTech Research*, vol. 1, no. 4, p. 354, 2009.
- [91] V. Vasconcelos Gomes de Oliveira *et al.*, "Study of acute oral toxicity of the thiazole derivative n-(1-methyl-2-methyl-pyridine)-n-(p-bromophenylthiazol-2-yl)-hydrazine in a syrian hamster," *Toxicology Mechanisms and Methods*, vol. 31, no. 3, pp. 197–204, 2021.
- [92] R. K. Nishad, K. A. Singh, and M. A. Rahman, "Synthesis and pharmacological activities of benzothiazole derivatives," *Indian Journal of Pharmaceutical Education and Research*, vol. 58, no. 3s, pp. s704–s719, 2024.
- [93] A. Rouf and C. Tanyeli, "Bioactive thiazole and benzothiazole derivatives," *European Journal of Medicinal Chemistry*, vol. 97, pp. 911–927, 2015.

- [94] A. Kumar and A. K. Mishra, "Advancement in pharmacological activities of benzothiazole and its derivatives: An up to date review," *Mini Reviews in Medicinal Chemistry*, vol. 21, no. 3, pp. 314–335, 2021.
- [95] A. Kamal, M. A. H. Syed, and S. M. Mohammed, "Therapeutic potential of benzothiazoles: a patent review (2010–2014)," *Expert Opinion on Therapeutic Patents*, vol. 25, no. 3, pp. 335–349, 2015.
- [96] R. Ali and N. Siddiqui, "Biological aspects of emerging benzothiazoles: a short review," *Journal of Chemistry*, vol. 2013, no. 1, p. 345198, 2013.
- [97] R. K. Gill, R. K. Rawal, and J. Bariwal, "Recent advances in the chemistry and biology of benzothiazoles," *Archiv der Pharmazie*, vol. 348, no. 3, pp. 155–178, 2015.
- [98] S. Agarwal, D. Gandhi, and P. Kalal, "Benzothiazole: A versatile and multi-targeted pharmacophore in the field of medicinal chemistry," *Letters in Organic Chemistry*, vol. 14, no. 10, pp. 729–742, 2017.